Universidad de Huelva

Departamento de Química y Ciencia de los Materiales

Design and characterization of molecular fluorescent architectures for potential applications as sensors and logic switches

Memoria para optar al grado de doctora
presentada por:

Vânia Cristina Fernandes Pais

Fecha de lectura: 30 de enero de 2014

Bajo la dirección del doctor:

Uwe Pischel

Huelva, 2014

DESIGN AND CHARACTERIZATION OF MOLECULAR FLUORESCENT ARCHITECTURES FOR POTENTIAL APPLICATIONS AS SENSORS AND LOGIC SWITCHES

A dissertation presented by
Vânia Cristina Fernandes Pais

Oriented by Dr. Uwe Pischel

to the University of Huelva in partial fulfillment of the requirements for the degree of
Doctor of Philosophy in Chemistry

University of Huelva
Huelva, December 2013

Committee:

_____

_____

_____

Statement of Originality

Hereby, I, Vânia F. Pais, certify that all results that are described and discussed in this thesis derive from my own work under the supervision of Dr. Uwe Pischel, with the following exceptions:

Chapter 2: The synthesis of the compounds was performed by Dr. Daniel Collado from the University of Málaga (Spain).

Chapter 3 and **Chapter 4:** The synthesis of the compounds and all NMR-spectroscopic characterization were performed by Dr. Abel Ros from the *Instituto de Investigaciones Químicas* (CSIC-US) Seville (Spain). The DFT calculations were carried out by Dr. Hamdy S. El-Sheshtawy from the South Valley University in Quena (Egypt).

Author: _____

Supervisor: _____

Date: _____

Acknowledgements

First of all I would like to thank my supervisor, Dr. Uwe Pischel, for his guidance, knowledge, and brilliant ideas. Without him I would not have achieved my goals for this dissertation. I also thank the *Junta de Andalucía*, for funding within the research project (F08-FQM-3685) and my doctoral fellowship.

I also would like to thank Dr. Abel Ros (University of Seville) and Dr. Daniel Collado (University of Málaga) for the synthesis of the compounds used in the presented papers.

A special acknowledgement goes to my two “old friends” of the laboratory, Cátia and Patricia, for their help, patience, and friendship, and to the other members of the group for the fruitful working environment.

I would like to thank my family, especially my parents Inácio and Maria, my brothers, sisters in law, nieces, and nephews for all their love and support.

Last but not least, I would like to thank my life partner, Gonçalo, for his help and encouragement during all the years and my beautiful daughter, Diana Pais Basílio, for her smile and unconditional love.

List of Papers Discussed in this Thesis

1- ***Off-On-Off Fluorescence Switch with T-Latch Function***
Pais, V. F.; Remón, P.; Collado, D.; Andréasson, J.; Pérez-Inestrosa, E.; Pischel, U. *Org. Lett.* **2011**, *13*, 5572-5575.

2- ***Borylated Arylisoquinolines: Photophysical Properties and Switching Behavior of Promising Tunable Fluorophores***
Pais, V. F.; El-Sheshtawy, H. S.; Fernández, R.; Lassaletta, J. M.; Ros, A.; Pischel, U. *Chem. Eur. J.* **2013**, *19*, 6650-6661.

3- ***Preparation and pH-Switching of Fluorescent Borylated Arylisoquinolines for Multilevel Molecular Logic***
Pais, V. F.; Lineros, M.; López-Rodríguez, R.; El-Sheshtawy, H. S.; Fernández, R.; Lassaletta, J. M.; Ros, A.; Pischel, U. *J. Org. Chem.* **2013**, *78*, 7949-7961.

Other Papers

4- ***Information Processing with Molecules—Quo Vadis*?**
Pischel, U.; Andréasson, J.; Gust, D.; Pais, V. F. *ChemPhysChem* **2012**, *14*, 28-46.

5- ***Unconventional Fluorescence Quenching in Naphthalimide-Capped CdSe/ZnS Nanoparticles***
Aguilera-Sigalat, J.; Pais, V. F.; Doménech-Carbó, A.; Pischel, U.; Galian, R. E.; Pérez-Prieto, J. *J. Phys. Chem. C* **2013**, *117*, 7365-7375.

6- ***Highly Sensitive Organic Molecular Fluorescent Thermometers Based on Borylated Arylisoquinolines***
Pais, V. F.; Lassaletta, J. M.; Fernández, R.; El-Sheshtawy, H. S.; Ros, A.; Pischel, U. *to be submitted*.

ISI Journal Citation Reports (Web of Science)

The works that form the basis of this PhD thesis are published in international peer-reviewed journals with high impact factors. In detail the following indicators can be found in the Web of Science for the three journals:

1- *Organic Letters* (*Org. Lett.*): Impact factor (2013): 6.142; Position (Organic Chemistry): 6 de 57.

2- *Chemistry – A European Journal* (*Chem. Eur. J.*): Impact Factor (2013): 5.831; Position (Chemistry Multidisciplinary): 21 de 152.

3- *The Journal of Organic Chemistry* (*J. Org. Chem.*): Impact Factor (2013): 4.564; Position (Organic Chemistry): 10 de 57.

As can be seen, all of them are located in the first quarter (Q1) of their respective fields.

List of Conferences

Note: The presenting authors are underlined.

1- ***Photophysical Studies of the Interaction of Nitroaniline Ligands with Quantum Dots***

Pais, V. F.; Pischel, U., Book of Abstracts *10th National Meeting of Photochemistry (10ENF)*, *Sociedade Portuguesa de Química*, December 9-10, **2010**, Porto, Portugal. (Poster)

2- ***A Molecular Logic Memory Device***

Pais, V. F.; Remón, P.; Collado, D.; Andréasson, J.; Pérez-Inestrosa, E.; Pischel, U., Book of Abstracts *III Jornadas Ibéricas de Fotoquímica and X Congreso de Fotoquímica*, September 4-7, **2011**, Granada, Spain. (Poster)

3- ***Pyridinium Porphyrins and Their Host-Guest Interactions with Cucurbituril Macrocycles***

Costa, D. C. S.; Pais, V. F.; Silva, A. M. S.; Cavaleiro, J. A. S.; Pischel, U.; Tomé, J. P. C., Book of Abstracts *3rd Portuguese Young Chemists Meeting (PYCHEM 2012)*, **2012**, May 9-11, Oporto, Portugal. (Poster)

4- ***OFF-ON-OFF Fluorescence Switch with T-Latch Function***

Pais, V. F.; Remón, P.; Collado, D.; Andréasson, J.; Pérez-Inestrosa, E.; Pischel, U., Book of Abstracts *XXIV IUPAC Symposium on Photochemistry*, July 15-20, **2012**, Coimbra, Portugal. (Poster)

5- ***Evaluation of Photoelectron Transfer in OFF-ON-OFF Fluorescence Switch***

Collado, D.; Najera, F.; Pérez-Inestrosa, E.; Pischel, U.; Pais, V. F.; Remón, P., Book of Abstracts *XXIV IUPAC Symposium on*

Photochemistry, July 15-20, **2012**, Coimbra, Portugal. (Oral Communication)

6- ***Amine-Induced Changes in the Optical Features of Naphthalimide Coated CdSe/ZnS Nanohybrids***

Aguilera-Sigalat, J.; Domenech, A.; Pais, V. F.; Pischel, U.; Galian, R. E.; Pérez-Prieto, J., Book of Abstracts *XXIV IUPAC Symposium on Photochemistry*, July 15-20, **2012**, Coimbra, Portugal. (Poster)

7- ***Pyridinone Phthalocyanines and Their Host-Guest Complexes with Cucurbit-7-uril***

Lourenço, L. M. O., Pais, V. F.; Neves, M. G. P. M. S.; Cavaleiro, J. A. S.; Pischel, U.; Tomé, J. P. C., Book of Abstracts *XXIII Encontro Nacional da SPQ*, June 12-14, **2013**, Aveiro, Portugal. (Poster)

8- ***Bor-ON or OFF: An Unexpected Discovery of a Versatile Class of Fluorescent Organoboron Switches and Their Applications***

Pischel, U.; Pais, V. F.; Ros, A.; Fernández, R.; Lassaletta, J. M.; El-Sheshtawy, H. S., Book of Abstracts *XXXIV Reunión Bienal de la Real Sociedad Española de Química*, September 15-18, **2013**, Santander, Spain. (Oral Communication)

Abstract

The increasing complexity of information technology and the therewith connected demands for miniaturization have alimented the need for alternative small-scale approaches to computing and data processing. Molecules can be one solution for this problem. However, they must be taught to integrate the functions of computing such as logic gates and circuits. Molecular switches can be converted from one state to another by a wide range of external stimuli, such as chemical species, light, temperature *etc*. This switching action can be translated into binary codes and in some cases (as shown in this thesis) also into multivalued coding. Beside their potential for computing, applications in object coding, intelligent materials, pro-drug activation, and diagnostics/actuation are widely pursued with molecular switches nowadays.

The global objective of this research is to develop new molecular systems, based on molecular logics. Particular attention is given here to aminonaphthalimides and arylisoquinoline dyes with boronic ester groups. The aminonaphthalimide fluorophore, integrated in a receptor$_1$-fluorophore-receptor$_2$ architecture, is able to switch its fluorescence upon application of acid input in an *off-on-off* manner. Thereby the characteristics of a T-latch function are mimicked with a molecular system. Furthermore, a new class of arylisoquinoline fluorophores with boronic ester groups was extensively investigated. The internal-charge-transfer (ICT) fluorescence emission of these dyes can be fine-tuned in an ample spectral window. These fluorophores can be switched by protonation of the isoquinoline moiety or the formation of fluoroboronate complexes with the boronic acid ester. Borylated arylisoquinoline dyes with pH-dependent fluorescence are also discussed. These dyes feature aromatic amino substitution with appended lateral aliphatic amino groups and the isoquinoline proton receptor. The photophysical properties of the ICT dyes were studied and the fluorescence modulation upon multiple and orthogonal protonation with acid led to the

interpretation of multi-level switching including *off-on-off*, ternary, and quaternary responses.

Resumen

La creciente complejidad de las tecnologías de información y las demandas relacionadas con las mismas con respecto a la miniaturización han aumentado la necesidad de enfoques a pequeña escala alternativos para la computación y el procesamiento de datos. Las moléculas pueden ser una solución para este problema. Sin embargo, deben ser "enseñados" a integrar las funciones de computación, tales como puertas lógicas y circuitos lógicos. El estado de los interruptores moleculares se puede modificar, intercambiar de ON a OFF, por medio de una amplia gama de estímulos externos, tales como especies químicas, la luz, la temperatura, etc. Esta acción de conmutación se puede traducir en códigos binarios y en algunos casos (como se muestra en esta tesis), también en codificación de varios valores. Junto a su potencial para aplicaciones de computación en la codificación de objetos, en la actualidad, también se consiguen con éxito otros sistemas por medio de interruptores moleculares, como son materiales inteligentes, activación pro-fármacos y diagnóstico/actuación.

El objetivo general de esta investigación es desarrollar nuevos sistemas moleculares, basados en la lógica molecular. Se presta especial atención a los derivados de aminonaftalimida con diferentes receptores amino y colorantes arilisoquinolina borilados con grupos éster borónico.

El fluoróforo aminonaftalimida, integrado en una arquitectura *receptor*$_1$-*fluoróforo-receptor*$_2$, es capaz de cambiar su fluorescencia, tras la aplicación de un ácido, de una manera *off-on-off*. De este modo se llegan a imitar las características de una función T-latch con un sistema molecular.

Además, se investigó extensamente una nueva clase de fluoróforos arilisoquinolina con grupos éster borónico. La transferencia interna de carga (TIC) de emisión de fluorescencia de los colorantes puede ser ajustada en una amplia ventana espectral. Estos fluoróforos se pueden conmutar por protonación de la fracción de isoquinolina o por la formación de complejos fluoroboronados con el éster de ácido borónico utilizando iones fluoruro.

También se discute sobre colorantes arilisoquinolina borilados con fluorescencia dependiente del pH. Estos colorantes cuentan con una sustitución amino aromático con grupos amino alifáticos laterales adjuntos y el receptor isoquinolina de protones. Se estudiaron las propiedades fotofísicas de la TIC y, la modulación de la fluorescencia tras la protonación múltiple y ortogonal con ácido, dio lugar a unos cambios en las señales que permitieron la interpretación de múltiples niveles incluyendo *off-on-off*, y respuestas ternarias y cuaternarias.

También se discuten colorantes arilisoquinolina borilados con fluorescencia dependiente del pH. Estos colorantes cuentan con una sustitución amino aromático con grupos amino alifáticos laterales adjuntos y el receptor isoquinolina de protones. Las propiedades fotofísicas de la transferencia interna de carga se estudiaron y la modulación de la fluorescencia tras la protonación múltiple y ortogonal con ácido llevó a una interpretación de conmutación de múltiples niveles incluyendo *off-on-off*, y respuestas ternarias y cuaternarias.

List of Figures

List of Schemes

List of Tables

Table of Contents

Chapter 1

Introduction

1. Introduction

The logic of computing is based on a binary system represented by two different values, ones and zeros. This concept relates to Boolean logic that is defined as a logical system of operators. The concept of logic is not only applied in the computer world, but it is valid for any system that can distinguish two or more states for the input and output signals. In other words, the concept of logic is universal. By implementation with molecular systems, for example photonic and chemical signals can be used for the processed signal (input) and for the answer signal (output). These cases will be discussed briefly in this introductory chapter.

1.1 Molecular Chemosensors

A molecular chemosensor is defined as chemical structure being able to bind an ionic or neutral guest species through supramolecular recognition by a receptor and producing a detectable change of the systems' state that can be read by means of a physical parameter. Besides reporting the presence of the guest species the receptor should be selective and also have the potential for information processing. In many (and the simplest) cases the physical properties can be switched between *off* and *on* states,[1] referring to magnetic, electronic, or luminescent properties. The external stimuli are called inputs and may comprise of ions (protons, metal cations or anions), neutral molecules, temperature, light irradiation, *etc*.
The sensing function at the molecular level can be achieved by conjugation of a reporter group to a binding site. The reporter group should be chosen according to its propensity to change electrochemical or spectroscopic properties upon recognition of the guest input by the receptor.

Fluorescence is one of the most common methods for the detection of analytes due to advantages such as fast response times, sensitivity, and often highly selective optical signatures. In fluorescent molecular chemosensors the fluorophore acts as a signal transducer that converts the input recognition by the receptor into an optical signal that derives from the changes of photophysical properties.[2] The communication between the fluorophore and the receptor unit is often achieved by excited state mechanisms such as internal charge transfer (ICT), energy transfer or photoinduced electron transfer (PET). A few examples for these principles (based on ICT and PET) in chemosensing are briefly outlined in the next paragraphs.

Usually, ICT states are observed in "push-pull" π-systems which integrate an electron-donating and an electron-withdrawing group.[3] In such systems light excitation leads to a redistribution of electron density, so that substantial dipole moment changes are observed. Commonly such states show large Stokes shifts and pronounced solvatochromic effects. Many ICT chromophores are fluorescent and upon binding of analytes the ICT states can be energetically stabilized or destabilized. This results commonly in spectral shifts of the emission (see Scheme 1.1).[4]

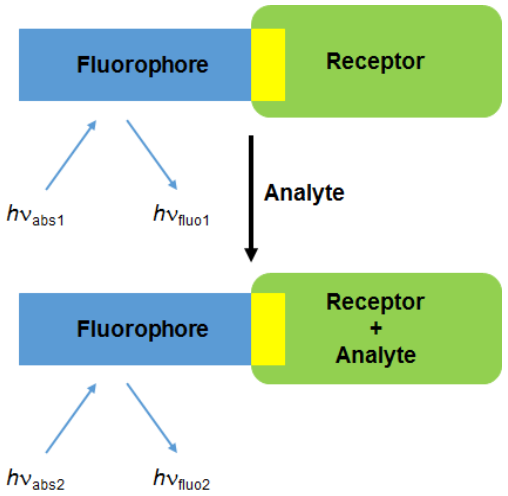

Scheme 1.1. Design of fluorescent ICT switches.[5]

Whether a blue shift or red shift is observed in the emission spectra depends on the positioning of the receptor.[5] When a receptor group is connected to the electron-donating terminal, the binding of a cation causes a reduction of the electron-donating character leading to a blue shift of the absorption and fluorescence spectra. On other hand, if the cation interacts with the electron-accepting group, then the ICT state is energetically stabilized and red-shifted absorption and fluorescence spectra are observed.[6]

A very simple example for the switching of an ICT fluorophore is the aminonaphthalimide **1** (Figure 1.1).[7] This system exhibits an intense green emission. The electron-donating amino (NH_2) group can interact with basic anions ($H_2PO_4^-$, OH^-), leading to deprotonation (OH^-) or hydrogen bonding interactions ($H_2PO_4^-$).[8,9] As a result a fluorescence quenching and a red shift of the emission band are observed. Deprotonation increases the electron density at the amino group making it an even better donor: red shift of emission. The addition of acid also leads to fluorescence quenching, presumably due to the protonation of the carbonyl oxygens.

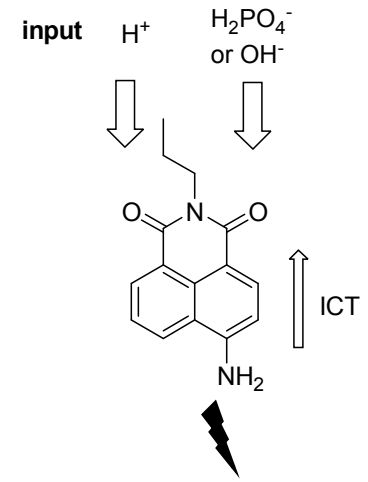

1

Figure 1.2. Structure and switching of the ICT fluorophore **1**.

Photoinduced electron transfer (PET) is one of the mostly used phenomena for the implementation of fluorescent chemosensors. In the majority of the cases the systems are designed to show fluorescence quenching due to PET from the receptor unit to the excited state fluorophore. Upon recognition of a chemical input by the receptor, the electronic properties of the latter are altered and the PET is blocked. This leads to fluorescence changes corresponding to *off-on* switching. The described situation is exposed in Scheme 1.2. In the initial state, corresponding to the absence of an analyte (or generally a chemical input species), the HOMO of the electron donor (corresponding to the receptor) is on a higher energy level than the acceptor's half-vacant HOMO (corresponding to the excited fluorophore) and PET occurs to the low-lying HOMO of the acceptor. This electron transfer provides a mechanism for non-radiative deactivation of the excited state giving a quenching of fluorescence and consequently a decreased emission quantum yield.[3] Upon analyte addition and the binding with the receptor unit of the sensor the donor HOMO falls energetically below the acceptor HOMO, thereby preventing electron transfer from the electron donor to the electron-accepting fluorophore. As a result the fluorescence is increased.

The preferred molecular design for this approach is based on the *fluorophore-spacer-receptor* architecture.[2,10] The spacer holds the fluorophore and receptor separate from each other and isolates both units electronically. The receptor is the unit responsible for the guest complexation, and the fluorophore is the signaling unit.

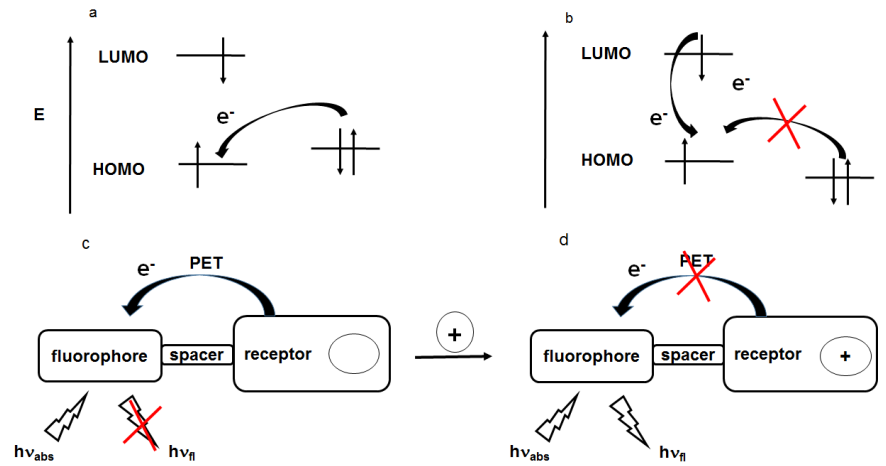

Scheme 1.2. Frontier orbital energy diagram for fluorescence switching by modulation of PET.[6]

Some examples for fluorescent chemosensors that are based on the PET mechanism are shown in Figure 1.2.

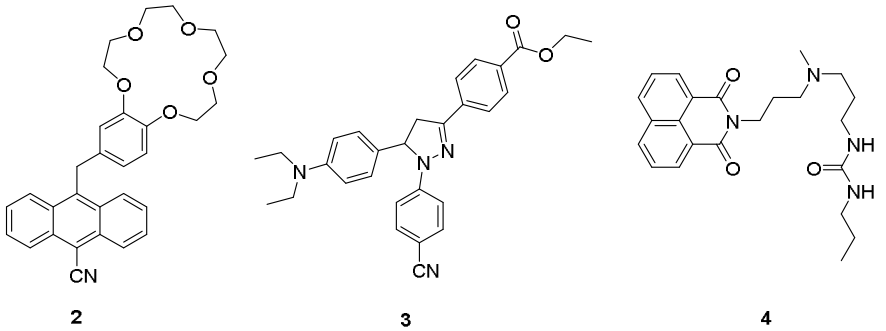

Figure 1.2. Fluorescent sensor based on PET.

Compound **2** represents a fluorescence sensor for Na^+ cations, reported by de Silva and coworkers,[11] while system **3** is a sensor for protons.[12] Compound **4** is a *fluorophore-spacer-receptor$_1$-spacer-receptor$_2$* conjugate which that can be used for the detection of protons or anions and that was also interpreted in terms of the modular functional integration of two-input INH molecular logic (see discussion of molecular logic below).[13] The system comprises of a 1,8-naphthalimide as fluorophore and electron-accepting unit and amino and urea receptors that can act as

electron donors in the absence (amino) or presence of analytes (anion-complexed urea). The system shows typical PET behavior.

The direction of the PET can be also inversed (excited fluorophore as electron donor and receptor as acceptor). Thus, in some cases the excited state fluorophore serves as electron donor and the occupied receptor as acceptor. This is often referred to as oxidative PET. Such behavior can be observed for the sensing of transition metal cations. This leads to *on-off* sensing systems. Examples are represented by the structures **5** and **6**, as shown in Figure 1.3.

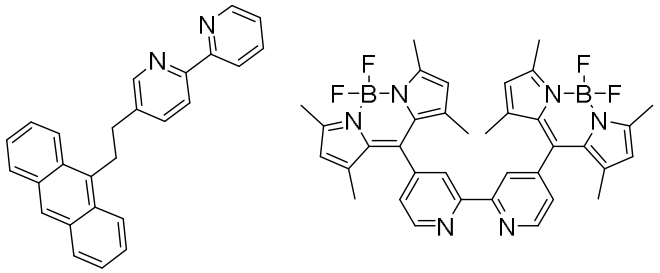

5 **6**

Figure 1.3. Oxidative PET sensors based on a 2,2′-bipyridyl receptor with anthracene (**5**) or a BODIPY dye (**6**) as fluorophores.

Compound **5**, which was reported by de Silva and co-workers, is an example for such an *on-off* sensor. It works with zinc ions or protons. The compound is fluorescent in the absence of these chemical inputs, but in their presence the bipyridyl unit turns into an electron acceptor and the anthracene signaling unit gets quenched by oxidative PET.[14]

Another example (**6**) was reported by the Akkaya group.[15] The represented system has a significant quantum yield (Φ_f = 0.39) in its uncomplexed state, but in the presence of zinc cations the fluorescence becomes quenched for the same motives as outlined before (oxidative PET).

1.2. Molecular Logic Gates: Systems with One Input

The beforehand discussed PET-based fluorescence sensors can be equally interpreted as YES and NOT logic gates. Here the input and output signal levels are re-defined in a binary manner: a binary 0 relates to an absent or low signal, while the binary 1 reports a high signal. This can be applied to the concentration of chemical input species as well as to the intensity of a fluorescence output signal. In terms of a YES logic gate (also called an IDENTITY gate) the following situation applies: only when the input is 1 the output is reported as well as 1, while the absence of an input (0) leaves the output low (0); see truth table in Table 1.1. This switching behavior is clearly fulfilled by the above discussed *off-on* fluorescence switches based on PET. The described condition is also satisfied by system **7** (see Figure 1.4) composed of an anthracene that is linked to an amino-containing receptor and where the addition of ions Zn^{2+} leads a fluorescence enhancement.[16]

On the other hand, an *on-off* fluorescence sensor describes the inverse situation. In the absence of input (0) a high fluorescence signal is observed (binary 1), while upon addition of the input (1) a fluorescence quenching results (binary 0); see truth table in Table 1.1. This integrates the situation of a NOT logic gate, also called an INVERTER. The anthracene-thiourea system (**8**; see Figure 1.4), used for the sensing of basic anions such as fluoride or acetate, performs as a NOT logic gate.[17]

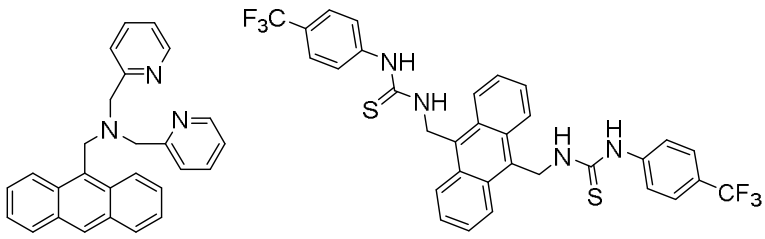

7 **8**

Figure 1.4. Example of a system which upon addition of Zn^{2+} ion performs a YES logic gate (**7**) and a system which performs as a NOT logic gate (**8**).

Table 1.1. Truth table of a YES and NOT logic gate.[18]

I	*O*	*O*
0	0	1
1	1	0
Logic Gate	**YES**	**NOT**

The described molecular logic gates are based on only one input and output, integrating a relatively trivial situation. However, the examples show very nicely the tight connection that exists between sensing and molecular logic. Beside the discussed systems more complex molecular logic functions with multiple inputs have been reported over the years. In fact, it was a two-input AND logic gate that constituted the first example of a fluorescent logic switch, reported by de Silva and co-workers in 1993.[19] In the following parts of this chapter I will discuss a few examples of molecular logic systems which show fluorescence (or generally optical) output signaling behavior as function of multiple chemical or photonic inputs.

1.3. Molecular Logic Gates: Two Inputs

As outlined above, the first example for molecular logic fluorescence switching by external stimuli that was interpreted in a binary manner has been known since 1993. In essence de Silva and his group demonstrated a photoionic AND gate.[19] For the two-input AND gate the output is high (binary 1) only when the two inputs are simultaneously high (binary 1). All other input combinations (00, 01, 10) give a 0 output. This is summarized in the truth table that is shown in Figure 1.5. The system presented by de Silva integrates a *fluorophore-spacer$_1$-receptor$_1$-spacer$_2$-receptor$_2$* architecture **9** (see Figure 1.5)

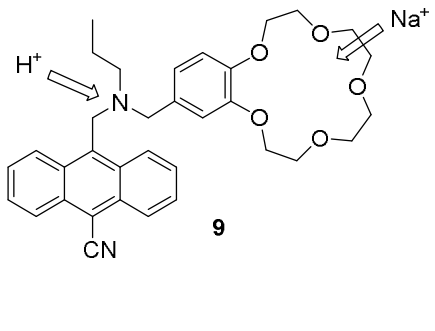

In1	*In2*	*Output*
0	0	0
0	1	0
1	0	0
1	1	1

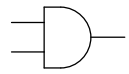

AND

Figure 1.5. Molecular system **9**, truth table, and electronic representation for an AND logic gate.

In the represented case, an anthracene is the fluorophore whose fluorescence is quenched by the two receptors. The quenching mechanism is PET involving a tertiary amino group and a dialkoxybenzene as electron-donating functions. The inputs are represented by the chemical species protons and sodium ions. This choice avoids cross reactivity, because protons are specific for the amino function, while the sodium ions only interact with the crown ether moiety. The simultaneous addition of the two chemical species blocks PET and leads to fluorescence increase of the anthracene signaling unit. If just one input is present then the unoccupied receptor still quenches the

fluorescence via PET. The same applies for the absence of chemical input, where both receptors act as fluorescence quenchers.

After this pioneering demonstration other essential two-input logic gates (see truth tables of the examples OR, INH, XOR, NOR, XNOR in Table 1.2) have been realized at molecular scale as well.

Table 1.2. Truth table for two input logic gates.[18]

I_1	I_2	*Output*					
0	0	0	0	0	0	1	1
0	1	0	1	1	1	0	0
1	0	0	1	0	1	0	0
1	1	1	1	0	0	0	1
Logic Gate		**AND**	**OR**	**INH**	**XOR**	**NOR**	**XNOR**

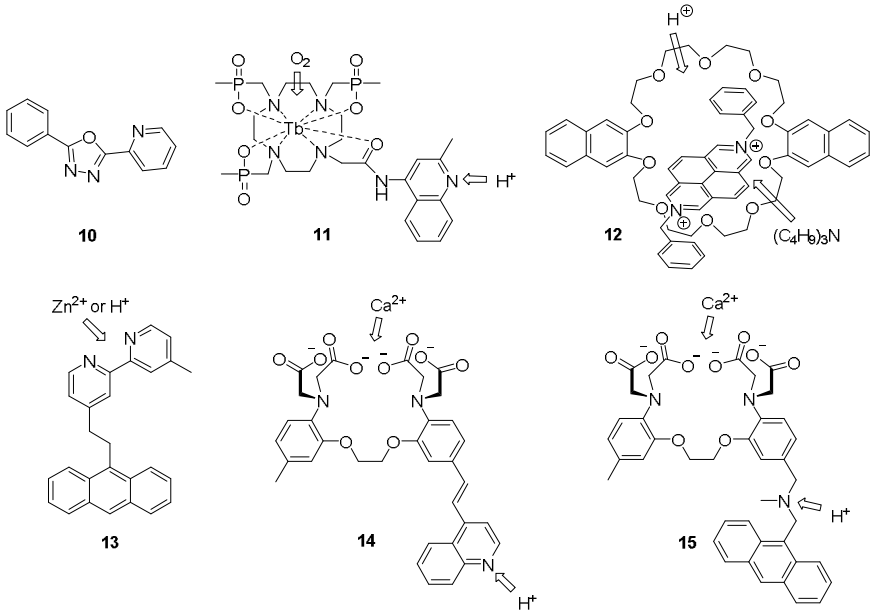

Figure 1.6. Molecular systems used for the demonstration of OR (**10**), INH (**11**), XOR (**12**), NOR (**13**), an XNOR/XNOR (**14**), and an AND (**15**) logic gate**.**

An OR logic gate produces a binary 1 output when at least one of the inputs is high (binary 1). Instead, if both inputs are 0 then the output is also 0. This kind of logic gate can be implemented with a non-selective receptor that gives an output for example in form of a fluorescence signal upon binding of either chemical species. A recent example is compound **10** (Figure 1.6) which is able to recognize two different metal cations (zinc and cadmium ions).[20] The presence of either cation or both induced a fluorescence enhancement of the molecule, due to metal ion binding to the 1,3,4-oxadiazole unit. Hence, the molecule behaves as an OR logic gate.

An AND gate, where one of the inputs is inverted, is considered an INHIBIT gate (INH). According to the truth table (see Table 1.2), only when the inverted input is 0 and the other one is 1, then the output corresponds to a binary 1. The other possible combinations result in a binary 0 output. In 2000, Gunnlaugsson, Parker and co-workers reported an example of an INH gate using the terbium complex **11** based on a macrocyclic 1,4,7,10-tetraazocyclododecane ligand with an appended quinoline substituent (Figure 1.6).[21] In presence of protons and in absence of oxygen, the emission band of the terbium at 548 nm was far more intense than in basic solution and in presence of O_2. For the other input combinations no emission was observed. The working principle was based on the energy-transfer-antenna effect of the quinoline moiety, which under specific conditions is able to sensitize the lanthanide luminescence.

The exclusive-OR gate (XOR) registers a high output value (binary 1) when exactly one of the two inputs is high (binary 1). In case of both inputs being high or low the output represents a low signal (binary 0). The implementation of such logic gate is not trivial, because the presence of both inputs has to yield an inverse result as compared to the presence of only either input.[22]

The in Figure 1.6 represented supramolecular system **12** is a pseudorotaxane with an electron-accepting 2,7-dibenzyldiazepyrenium dication as thread and a crown ether with two electron-donating 2,3-

dioxynaphthalene units as ring.[22] The charge-transfer interaction between the electron-accepting and electron-donating parts of the assembly enables the formation of a pseudorotaxane which is accompanied by fluorescence quenching of the naphthalene chromophore. The addition of competitively binding protons or tri-*n*-butylamine resulted in a fluorescence enhancement which is motivated by the de-threading of the aromatic dication. The simultaneous presence of the two inputs caused acid-base neutralization, thereby regenerating again the pseudorotaxane assembly with the consequent observation of fluorescence quenching. The described molecular behavior is compatible with XOR logic.

The logic gates NOR and XNOR (exclusive NOR) can be understood as inverted OR or XOR gates, respectively. Hence, in a NOR gate the output is only obtained as a binary 1 if the two inputs are 0. The addition of zinc cations, protons or both at the same time to the compound **13** turned the fluorescence *off*.[14] Thus, only in absence of inputs the fluorescence remained high, in accordance with a NOR operation.

For a XNOR gate the outputs are a binary 1 when the inputs are of the same value (0 or 1) and binary 0 when the inputs are different (for the two-input situations 01 and 10). The compound **14** has a quinoline group (receptor for protons) and a receptor unit for calcium ions.[23] This system represents an XNOR gate if transmittance at 390 nm is read as output.

1.4. Advanced Molecular Logic Circuits

Beside the above discussed simple two-input logic gates many more complex logic circuits were realized with molecular systems over the last decade. Among them are half-adders and half-subtractors,[24-26] multiplexers/demultiplexers,[27-29] encoders/decoders,[30,31] keypad locks,[32-35] latches/flip-flops,[36-42] and multivalued logic devices.[43] Some of these developments will be briefly illustrated with some selected examples in the following paragraphs.

Half-adders (HA) are digital circuits that perform the addition of two binary digits. The HA is based on a combination of an XOR and an AND gate. The system is able to perform four operations: “0+0=00”, “0+1=01”, “1+0=01” and “1+1=10”, which are shown in Table 1.3. An HA operates with two inputs (I_1 and I_2) and generates two outputs that represent the carry (*C*) and the sum (*S*) outputs of the HA. Here the sum is described by the XOR gate and the carry digit is generated by an AND gate. The first molecular system that performed this arithmetic logic operation was published by de Silva and co-workers in 2000.[23] Their system corresponded to a “cocktail” of two molecules, each one representing the operation of one of the logic gates that are necessary for a HA. The XOR gate was represented by compound **14**, while compound **15** implemented the AND gate (Figure 1.6). The gates were operated based on the control of ICT and PET phenomena. A unimolecular HA (having the XOR and AND functions integrated in one molecule) was reported in 2003 by the group of Zhu/Zhang.[44] For this purpose the authors used a photochromic spiropyran (**16**) with UV light and Fe^{3+} ions as inputs; see Figure 1.7.[45]

Table 1.3. Truth table of a half-adder.[18]

I_1	I_2	O_1 AND (*C*)	O_2 XOR (*S*)	Binary sum	10-Base sum
0	0	0	0	00	0
0	1	0	1	01	1
1	0	0	1	01	1
1	1	1	0	10	2

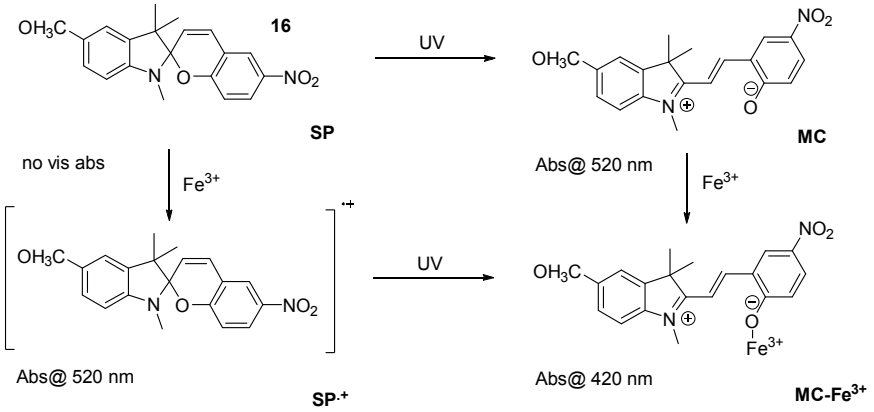

Figure 1.7. Structures of different states in the logic switching of spiropyran **16**.

The spiro (SP) form does not show absorption in the visible spectral range. However, when this form was exposed to UV light an isomerization to the merocyanine (MC) form took place, showing a new absorption band at 520 nm. When Fe^{3+} was added to the SP, the absorption at 520 nm increased due to the oxidation of SP to $SP^{\bullet+}$. When this form was exposed to UV light, the MC-Fe^{3+} was generated and an absorption band at 420 nm appeared, while the absorption band at 520 nm was practically inexistent. The same happened when the MC form was exposed to Fe^{3+} ions. The interpretation of the HA was possible by monitoring the absorbances at 420 nm and 520 nm as outputs for the AND and the XOR gate, respectively.

A half-subtractor (HS) has two inputs, I_1 (minuend) and I_2 (subtrahend), and two outputs, *D* (difference) and *B* (borrow). The borrow output *B* is described by an INH logic gate and the difference corresponds to the output of an XOR logic gate. The HS performs four operations according to: “0-0=00”, “1-0=01”, “0-1=11” and “1-1=00”; see Table 1.4.

Table 1.4. Truth table of a half-subtractor.[18]

I_1	I_2	O_1 INH (B)	O_2 XOR (D)	Binary difference	10-Base difference
0	0	0	0	00	0
0	1	1	1	01	1
1	0	0	1	11	-1
1	1	0	0	00	0

Langford and co-workers reported a HS based on the tetraphenyl-substituted free base porphyrin **17** and acid (HCl) or/and base (*t*-BuOK) as chemical inputs.[45,46] The working principle is shown in Figure 1.8.

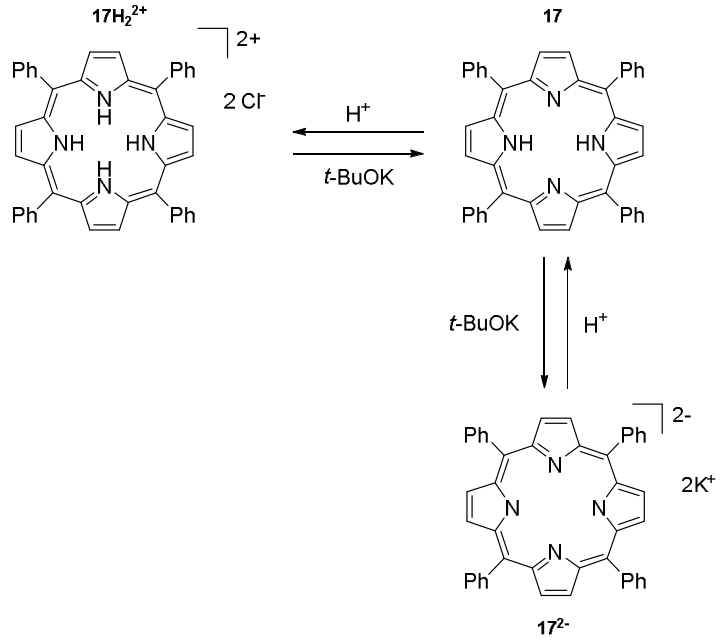

Figure 1.8. Structures of the different states upon input application with porphyrin **17**.

Porphyrin **17** has a Soret band at 417 nm, but when acid was added, resulting in the formation of **17H$_2^{2+}$**, this absorption band became practically zero. The same happened when base was added and the **17^{2-}**

dianion was formed. However, if the base and acid were added simultaneously the absorbance at 417 remained high, due to the neutralization of the two inputs. Hence, by monitoring the transmittance at 417 nm an XOR gate was obtained. The emission signal at 637 nm was used to integrate the INH gate. Here the output signal was highest for the presence of base and absence of acid.

Finally, in 2005 Shanzer and co-workers reported a case where a unimolecular platform was shown to integrate both the half-adder and the half-subtractor.[47] This device is also called moleculator. Surprisingly, the simple pH indicator fluorescein (**18**) was sufficient to fulfill this complex task. Fluorescein exists in four different protonation states which have different UV/vis spectra. The neutral fluorescein **18** has an absorption band at 434 nm (pH 3.3), and the monoprotonated cationic form $\mathbf{18}^{+}$ at 437 nm (pH < 2). The anionic form $\mathbf{18}^{-}$ has absorption bands at 453 nm and 472 nm, while the deprotonated form ($\mathbf{18}^{2-}$) exhibits a band near 490 nm; they were stable at pH 5.5 and pH > 8, respectively. The HA was realized using degenerate base inputs, monitoring the absorbance at the wavelengths of 447 nm (XOR gate) and 501 nm (AND gate) as outputs. The neutral form was set as initial situation. The output observation wavelengths were chosen according the implementation of the required functions. For the HS implementation, also degenerate base inputs were used. The HS was realized by reading the absorption at 447 nm (XOR gate) and 474 nm (INH) gate. Interestingly, the system can be reset by a simple acid-base neutralization reaction.

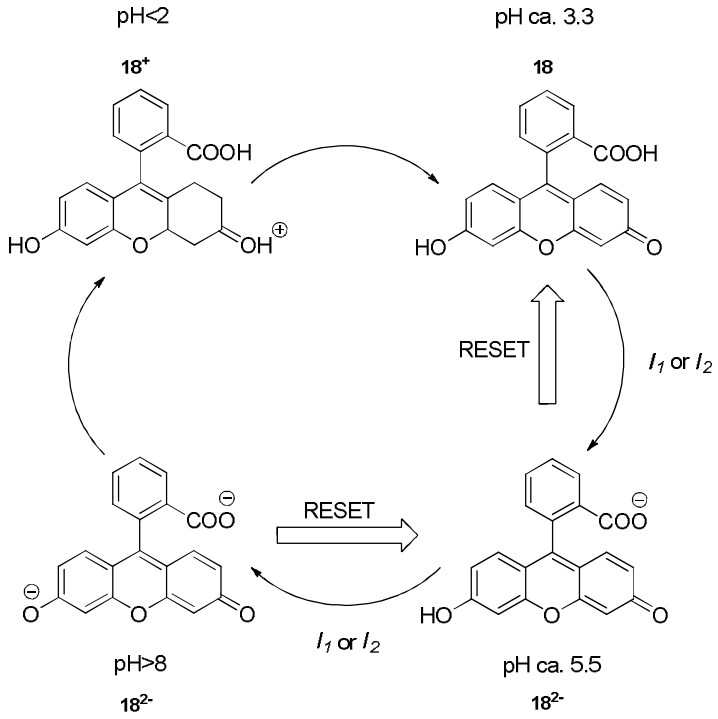

Figure 1.9. Different protonation states of fluorescein (**18**) and implication of three of them in the HA, where $I_1 = OH^-$, $I_2 = OH^-$ and RESET= H^+.

The described moleculator functions do not require to setup each logic gate (for example an XOR and an AND gate) with a separate molecule (physical integration). Rather the molecules work via functional integration and the global molecular behavior is interpreted in terms of a multi-logic-gate circuit. The concept of functional integration is very specific for molecular logic. De Silva and McClenaghan reported in 2002 an example for functional integration with a receptor$_1$-ICT chromophore-receptor$_2$ conjugate (**19**).[48] By using acid and cations (Ba^{2+} and Sr^{2+}) as chemical inputs and monitoring the transmittance of the solution at 402 nm it was possible to mimic a circuit composed of two concatenated logic gates: an XOR and an OR gate. However, none of these gates was separately implicated through a specific molecular species, leading thereby to the description of functional integration. The complete system reacts to the inputs as if it would be corresponding to the described logic circuit.

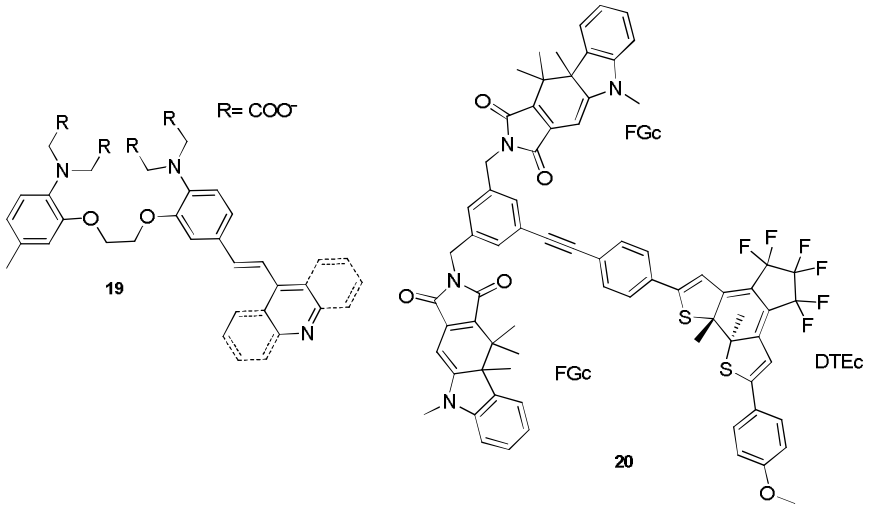

Figure 1.10. Molecular examples for the functional integration of logic functions.

However, arithmetic data processing is only one of the advanced logic operations that have been realized with molecular entities. In 2011 the groups of Andréasson, Pischel, and Gust published a triad (**20**) that is composed of two types of photochromic switches: fulgimide (FG) and dithienylethene (DTE); see Figure 1.10. The two photochromes can be addressed by different wavelengths in an independent manner. The resulting photochromic network is shown in Scheme 1.3.

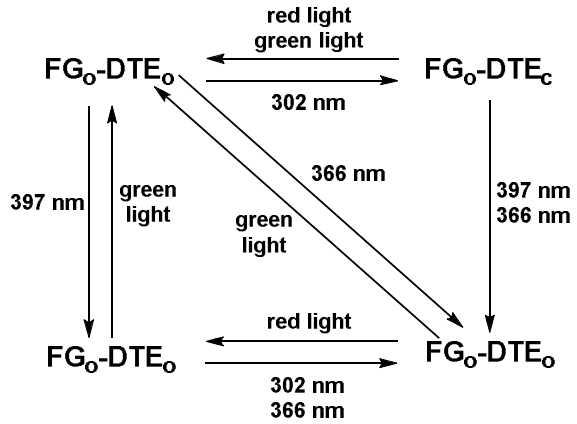

Scheme 1.3. Photochromic interconversions of triad **20**.

The different isomeric forms (only forms with the fulgimide photochrome in the same state are considered) of the triad feature well differentiated UV/vis absorption and fluorescence properties. Thus, the selective isomerization of one or both photochrome types allows the realization of several combinatorial and sequential logic operations. Using three different inputs in the ultraviolet region (302, 366 and 397 nm) and also visible light irradiation (red and green light) together with output readings at five different wavelengths it was shown that the triad can perform the functions of thirteen (!) logic devices (among them half-adder, half-subtractor, multiplexer, demultiplexer, encoder, decoder, keypad lock, and reversible logic gates).[49] All functions operated with the FG_o-DTE_o isomer as initial state. Resetting from any state of operation was possible by green light irradiation. Another advantage of the system is its all-photonic operation. Thereby the reversible interconversion between the different states is possible without the accumulation of chemical waste (as observed for acid-base addressed systems).

The outputs of the logic devices described above are only dependent on the actual inputs. These logic systems are commonly referred to as combinational logic devices. Sequential logic circuits differ from combinatorial logic in that the output of the logic device is not only dependent on the present inputs, but also on past inputs. This means that the system stores information of the input history. The first molecular example of sequential logic is the photochemical keypad lock described by the Shanzer group.[50] The system is a Fe^{3+} complex of a fluorescein-linker-pyrene dyad (**21**); see Figure 1.11.

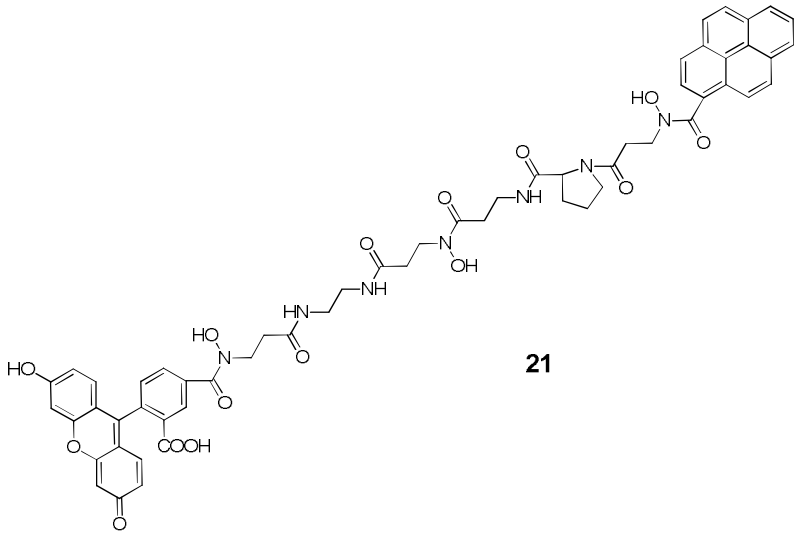

21

Figure 1.31. Structure of the dyad **21**.

The same function of a keypad lock was later demonstrated with the triad **20**. As inputs UV light at 366 nm and red light were used. The open state of the lock was signalized by fluorescence emission at 624 nm (originating from FG_c). It is important to mention that this fluorescence emission is only observed when the neighboring DTE is in its open form (DTE_o). Otherwise an efficient energy transfer to the closed DTE form quenches the emission of the FG_c. When FG_o-DTE_o was first irradiated with red light and then with UV light, the triad isomerized to the non-fluorescent FG_c-DTE_c form (lock closed). Instead using first UV light followed by red light led to the fluorescent FG_o-DTE_o isomer, corresponding to the open lock; see also the photochromic network shown in Scheme 1.3. Hence only the right order of input application opens the lock as it is also the case for “real life” keypad locks. The principle is also illustrated in Figure 1.12.

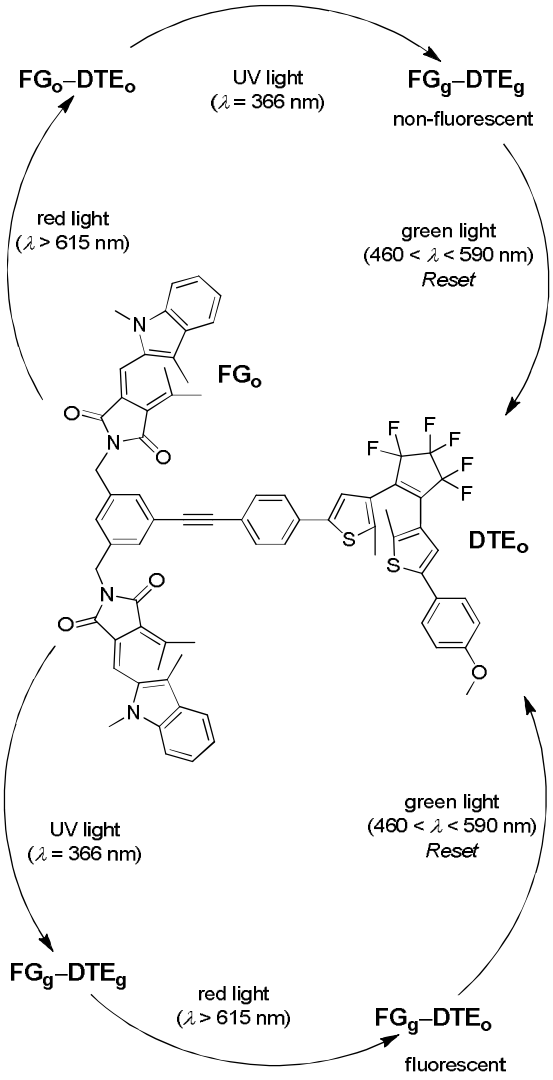

Figure 1.12. Working principle of a molecular keypad lock based on triad **20**.

This discussion closes the brief introduction to sensing and molecular logic. Much more could be written about this subject. However, the intention was to give a conceptual introduction and exposing few selected examples instead of reviewing the field in a comprehensive manner. At this point a series of excellent review articles and books, that cover especially the field of molecular logic, should be mentioned.[1,18,26,51-53] What should have become clear by now is that there is a straight

connection between fluorescent chemosensing, switching, and molecular logic. Exactly in this context the published works,[36,54,55] that are briefly discussed in the following chapters and that form the fundament of this cumulative thesis, have been developed. Additional bibliographic information can be found in the initial parts of the Chapters 3, 4, and 5, as well as in the corresponding publications.

1.5. References

[1] de Silva, A. P. *Molecular Logic-based Computation*; The Royal Society of Chemistry: Cambridge, **2013**.

[2] de Silva, A. P.; McCaughan, B.; McKinney, B. O. F.; Querol, M. *Dalton Trans.* **2003**, 1902.

[3] Valeur, B. *Molecular Fluorescence: Principles and Applications*; 1st ed.; Wiley-VCH: Weinheim, **2001**.

[4] Demchenko, A. P. *Introduction to Fluorescence Sensing*; Springer, **2008**.

[5] de Silva, A. P.; Fox, D. B.; Moody, T. S.; Weir, S. M. *Trends Biotechnol.* **2001**, *19*, 29.

[6] de Silva, A. P.; Gunaratne, H. Q. N.; Gunnlaugsson, T.; Huxley, A. J. M.; McCoy, C. P.; Rademacher, J. T.; Rice, T. E. *Chem. Rev.* **1997**, *97*, 1515.

[7] Remón, P.; Ferreira, R.; Montenegro, J.-M.; Suau, R.; Pérez-Inestrosa, E.; Pischel, U. *ChemPhysChem* **2009**, *10*, 2004.

[8] Gunnlaugsson, T.; Kruger, P. E.; Jensen, P.; Pfeffer, F. M.; Hussey, G. M. *Tetrahedron Lett.* **2003**, *44*, 8909.

[9] Pfeffer, F. M.; Seter, M.; Lewcenko, N.; Barnett, N. W. *Tetrahedron Lett.* **2006**, *47*, 5241.

[10] Callan, J. F.; de Silva, A. P.; Magri, D. C. *Tetrahedron* **2005**, *61*, 8551.

[11] de Silva, A. P.; Vance, T. P.; West, M. E. S.; Wright, G. D. *Org. Biomol. Chem.* **2008**, *6*, 2468.

[12] Fahrni, C. J.; Yang, L.; VanDerveer, D. G. *J. Am. Chem. Soc.* **2003**, *125*, 3799.

[13] Kluciar, M.; Ferreira, R.; de Castro, B.; Pischel, U. *J. Org. Chem.* **2008**, *73*, 6079.

[14] de Silva, A. P.; Dixon, I. M.; Gunaratne, H. Q. N.; Gunnlaugsson, T.; Maxwell, P. R. S.; Rice, T. E. *J. Am. Chem. Soc.* **1999**, *121*, 1393.

[15] Turfan, B.; Akkaya, E. U. *Org. Lett.* **2002**, *4*, 2857.

[16] de Silva, S. A.; Zavaleta, A.; Baron, D. E.; Allam, O.; Isidor, E. V.; Kashimura, N.; Percarpio, J. M. *Tetrahedron Lett.* **1997**, *38*, 2237.

[17] Martínez-Máñez, R.; Sancenón, F. *Chem. Rev.* **2003**, *103*, 4419.

[18] de Silva, A. P.; Uchiyama, S. *Nat. Nanotechnol.* **2007**, *2*, 399.

[19] de Silva, A. P.; Gunaratne, H. Q. N.; McCoy, C. P. *Nature* **1993**, *364*, 42.

[20] Li, A.-F.; Ruan, Y.-B.; Jiang, Q.-Q.; He, W.-B.; Jiang, Y.-B. *Chem. Eur. J.* **2010**, *16*, 5794.

[21] Gunnlaugsson, T.; Mac Donail, D. A.; Parker, D. *Chem. Commun.* **2000**, 93.

[22] Credi, A.; Balzani, V.; Langford, S. J.; Stoddart, J. F. *J. Am. Chem. Soc.* **1997**, *119*, 2679.

[23] de Silva, A. P.; McClenaghan, N. D. *J. Am. Chem. Soc.* **2000**, *122*, 3965.

[24] Bozdemir, O. A.; Guliyev, R.; Buyukcakir, O.; Selcuk, S.; Kolemen, S.; Gulseren, G.; Nalbantoglu, T.; Boyaci, H.; Akkaya, E. U. *J. Am. Chem. Soc.* **2010**, *132*, 8029.

[25] Margulies, D.; Melman, G.; Shanzer, A. *J. Am. Chem. Soc.* **2006**, *128*, 4865.

[26] Pischel, U. *Angew. Chem. Int. Ed.* **2007**, *46*, 4026.

[27] Amelia, M.; Baroncini, M.; Credi, A. *Angew. Chem. Int. Ed.* **2008**, *47*, 6240.

[28] Andréasson, J.; Straight, S. D.; Bandyopadhyay, S.; Mitchell, R. H.; Moore, T. A.; Moore, A. L.; Gust, D. *J. Phys. Chem. C* **2007**, *111*, 14274.

[29] Pérez-Inestrosa, E.; Montenegro, J.-M.; Collado, D.; Suau, R. *Chem. Commun.* **2008**, 1085.

[30] Andréasson, J.; Straight, S. D.; Moore, T. A.; Moore, A. L.; Gust, D. *J. Am. Chem. Soc.* **2008**, *130*, 11122.

[31] Ceroni, P.; Bergamini, G.; Balzani, V. *Angew. Chem. Int. Ed.* **2009**, *48*, 8516.

[32] Guo, Z. Q.; Zhu, W. H.; Shen, L. J.; Tian, H. *Angew. Chem. Int. Ed.* **2007**, *46*, 5549.

[33] Andréasson, J.; Straight, S. D.; Moore, T. A.; Moore, A. L.; Gust, D. *Chem. Eur. J.* **2009**, *15*, 3936.

[34] Remón, P.; Hammarson, M.; Li, S.; Kahnt, A.; Pischel, U.; Andréasson, J. *Chem. Eur. J.* **2011**, *17*, 6492.

[35] Strack, G.; Ornatska, M.; Pita, M.; Katz, E. *J. Am. Chem. Soc.* **2008**, *130*, 4234.

[36] Pais, V. F.; Remón, P.; Collado, D.; Andréasson, J.; Pérez-Inestrosa, E.; Pischel, U. *Org. Lett.* **2011**, *13*, 5572.

[37] Baron, R.; Onopriyenko, A.; Katz, E.; Lioubashevski, O.; Willner, I.; Wang, S.; Tian, H. *Chem. Commun.* **2006**, 2147.

[38] de Ruiter, G.; Motiei, L.; Choudhury, J.; Oded, N.; van der Boom, M. E. *Angew. Chem. Int. Ed.* **2010**, *49*, 4780.

[39] de Ruiter, G.; Tartakovsky, E.; Oded, N.; van der Boom, M. E. *Angew. Chem. Int. Ed.* **2010**, *49*, 169.

[40] Pischel, U. *Angew. Chem. Int. Ed.* **2010**, *49*, 1356.

[41] Pischel, U.; Andréasson, J. *New J. Chem.* **2010**, *34*, 2701.

[42] Remón, P.; Bälter, M.; Li, S. M.; Andréasson, J.; Pischel, U. *J. Am. Chem. Soc.* **2011**, *133*, 20742.

[43] Ferreira, R.; Remón, P.; Pischel, U. *J. Phys. Chem. C* **2009**, *113*, 5805.

[44] Guo, X. F.; Zhang, D. Q.; Zhang, G. X.; Zhu, D. B. *J. Phys. Chem. B* **2004**, *108*, 11942.

[45] Langford, S. J.; Yann, T. *J. Am. Chem. Soc.* **2003**, *125*, 14951.

[46] Langford, S. J.; Yann, T. *J. Am. Chem. Soc.* **2003**, *125*, 11198.

[47] Margulies, D.; Melman, G.; Shanzer, A. *Nat. Mater.* **2005**, *4*, 768.

[48] de Silva, A. P.; McClenaghan, N. D. *Chem. Eur. J.* **2002**, *8*, 4935.

[49] Andréasson, J.; Pischel, U.; Straight, S. D.; Moore, T. A.; Moore, A. L.; Gust, D. *J. Am. Chem. Soc.* **2011**, *133*, 11641.

[50] Margulies, D.; Felder, C. E.; Melman, G.; Shanzer, A. *J. Am. Chem. Soc.* **2007**, *129*, 347.

[51] Szaciłowski, K. *Chem. Rev.* **2008**, *108*, 3481.

[52] Andréasson, J.; Pischel, U. *Chem. Soc. Rev.* **2010**, *39*, 174.

[53] Pischel, U.; Andréasson, J.; Gust, D.; Pais, V. F. *ChemPhysChem* **2013**, *14*, 28.

[54] Pais, V. F.; El-Sheshtawy, H. S.; Fernández, R.; Lassaletta, J. M.; Ros, A.; Pischel, U. *Chem. Eur. J.* **2013**, *19*, 6650.

[55] Pais, V. F.; Lineros, M.; López-Rodríguez, R.; El-Sheshtawy, H. S.; Fernández, R.; Lassaletta, J. M.; Ros, A.; Pischel, U. *J. Org. Chem.* **2013**, *78*, 7949.

Chapter 2

Objectives

2. Objectives

The general objectives of this thesis are focused on the realization of new molecular switches that can find potential applications as fluorescent sensors and logic devices. Special interest has the implementation of multivalued logic where information processing is realized by ternary or quaternary logic. For this purpose the following specific objectives are:

- Design of an aminonaphthalimide-based receptor$_1$-fluorophore-receptor$_2$ architecture for the realization of *off-on-off* switching and the implementation of a logic device with the characteristics of a T-latch

- Design and photophysical investigation of boron-containing fluorophores based on arylisoquinolines with the possibility of fluorescence switching via protonation and/or fluoride binding

- Design and photophysical investigation of boron-containing fluorophores based on arylisoquinolines with the possibility to switch via orthogonal protonation; demonstration of ternary and quaternary logic (generally multivalued logic)

Chapter 3

A Molecular Logic T-Latch Memory Device

3. A Molecular Logic T-Latch Memory Device

This chapter is based on the manuscript:

OFF-ON-OFF Fluorescence Switch With T-Latch Function

Pais, V. F.; Remón, P.; Collado, D.; Andréasson, J.; Pérez-Inestrosa, E.; Pischel, U. *Org. Lett.* **2011**, *13*, 5572-5575.

3.1 Introduction

Recently, the design and synthesis of novel molecular logic devices has attracted significant research interest because these systems can be applied for the development of molecular computing.[1-3] However, also more immediate applications of this conceptual approach in clinical diagnosis,[4-6] pro-drug activation,[7-9] and the design of smart materials [10-12] have emerged recently.

One main objective of researchers is to develop systems that are capable of working as sequential logic devices or that perform complex logic functions such as adders/subtractores, endcoders/decoders, multiplexers/demultiplexers.[1,13-17]

In this chapter a sequential logic system, which is able to process two degenerate chemical inputs (protons) and that delivers fluorescence outputs will be briefly described. Its function resembles the behavior of a T-latch.

3.2 Molecular Design

In this work a new fluorescent triad with an integrated receptor$_1$-fluorophore-receptor$_2$ architecture was studied. The triad comprises of a 4-amino-substituted naphthalimide derivative as fluorophore, a quinoline unit at the imide side, and an electron-donating *N*-methylpiperazine unit at the aromatic 4-position of the imide. The quinoline and *N*-methylpiperazine units are both working as potential acceptors for proton inputs.

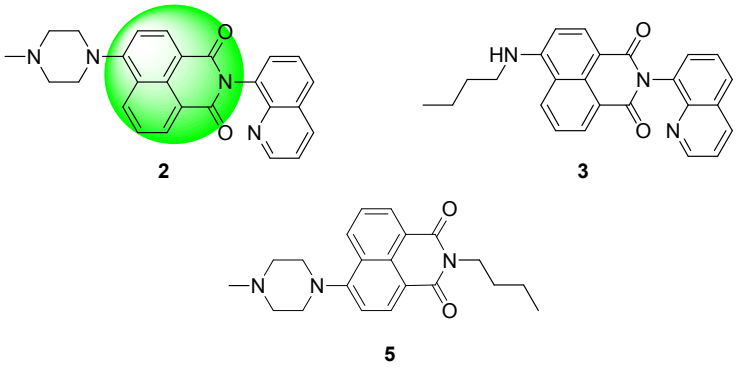

Scheme 3.1. Structures of compound **2** and the models **3** and **5**. Note that the numbering corresponds to the article on which this chapter is based (see Appendix A).

To understand the independent actuation of both receptors in compound **2**, two model compounds **3** and **5**, which contain each only one of the two receptors, quinoline or *N*-methylpiperazine, respectively, were investigated (Scheme 3.1).

The synthesis is described in the experimental section of the Supporting Information of the corresponding article (Appendix A1) and the photophysical characterization and implementation of the logic memory function will be briefly summarized in this chapter.

3.3 Photophysical Characterization

The photophysical properties of all investigated compounds and their protonated forms are summarized in Table 3.1.

Table 3.1. Photophysical properties of the compounds **2**, **3**, and **5** and their protonated forms in aerated acetonitrile solution.

	$\lambda_{abs,\,max}$/ nm	ε/ $M^{-1}cm^{-1}$	$\lambda_{fluo,\,max}$/ nm	Φ_f	τ_f/ ns
2	401	10100	504	0.017	[a]
2H$^+$	377	10500	499	0.67	8.90
2H$_2^{2+}$	383	11100	499	0.017	[a]
3	433	13000	520	0.56	10.00
3H$^+$	441	13400	519	0.006	[a]
5	398	9700	502	0.018	[a]
5H$^+$	374	10100	498	0.62	9.06

[a] Not determined due to low signal intensity.

In acetonitrile, compound **2** and the models **3** and **5** show their major UV/vis absorption bands in the region of 390-440 nm (Figure 3.1). Dyad **2** exhibits a band with a maximum at 401 nm (ε = 10100 $M^{-1}cm^{-1}$). The corresponding long-wavelength maxima for the models **3** and **5** were encountered at 433 nm (ε = 13000 $M^{-1}cm^{-1}$) and 398 nm (ε = 9700 $M^{-1}cm^{-1}$), respectively. The protonation of the piperazinyl residue leads to a blue shift by 24 nm of the aminonaphthalimide absorption band for the compounds **2** and **5**. This is a sign for the destabilization of the emissive charge-transfer state of the chromophore through the repulsive interaction between the protonated methyl-substituted N of the piperazinyl moiety and the partially positively charged N at the aryl residue.[18] On other hand, the protonation of the quinolinyl moiety leads to a red shift (6-8 nm) of the band of the naphthalimide for compound **2** and **3** due to stabilizing effects of the charge-transfer state.

The fluorescence spectra of all species (non-protonated or protonated) are dominated by a red-shifted and broad emission band in the region of 500-520 nm (Figure 3.1). For the compounds **2H$^+$** and **5H$^+$** the fluorescence quantum yield is high (Φ_f ca. 0.6-0.7) due to the protonation of the piperazinyl unit and consequently due to blocking of photoinduced electron transfer (PET). For the non-protonated compounds **2** and **5**, the quantum yields are lower than 0.02. Compound **3** exhibits a large fluorescence quantum yield (Φ_f = 0.56), that is explained by the absence of an electron-donating piperazinyl moiety that would lead to PET quenching. However, the protonation at the quinoline unit leads to a remarkable fluorescence quenching that is also observed for the analogous situation involving **2H$^+$**.

The fluorescence lifetimes were only measureable for **2H$^+$**, **3**, and **5H$^+$** (see Table 3.1) due to the low emission quantum yields in all other cases.

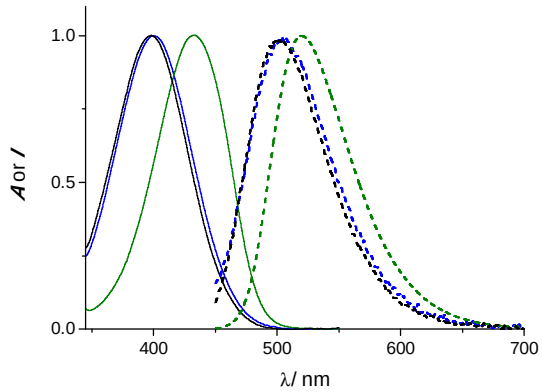

Figure 3.1. UV/vis absorption (solid lines) and fluorescence spectra (dashed lines) of the compounds in acetonitrile; blue: **2**, green: **3**, black: **5**.

3.4 T-Latch Function

There are many examples of fluorescent compounds in the literature that by addition of chemical species work as chemical sensors or logic switches.[2,19-22] Fluorescence as output signal has enjoyed preference in

the research community due to its easy detection and modulation via well controllable photophysical processes such as PET or energy transfer. The dye **2**, represented above, is an example of a system where emission properties change upon application of protons. Moreover, this system remembers its current state ($Q_{current}$) and the addition of another input gives a differentiated fluorescence output depending on the current state of the system. In detail, dye **2** functions as a logic device with memory function following the switching pattern of a so-called T-latch. Its working principle can be explained with the function of a conventional light switch (Scheme 3.2).

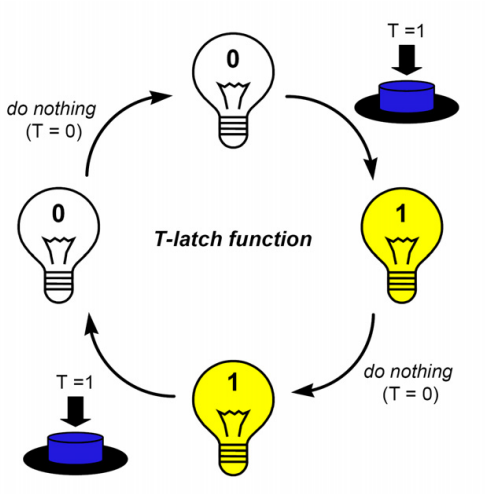

Scheme 3.2. Presentation of the T-latch function using the example of a light switch.

Every time the toggle input *T* is activated (*T* = 1) the state *Q* of the system changes between 0 and 1 or *vice versa*. Hence, if a 0 or a 1 state was memorized ($Q_{current}$), upon the following *T* input application the next state (Q_{next}) has the opposite value (0→1 and 1→0). The system remains in the hold state ($Q_{current} = Q_{next}$) in absence of input (*T* = 0). From the above analysis the truth table (Table 3.2) for the implementation of the T-latch is obtained.

Table 3.2. Truth table for the implemented molecular T-latch.

T input (1 equiv. H^+)	$Q_{current}$ (fluo)	Q_{next} (fluo)	*control channel* (abs, 313 nm)
0	0	0	0
1	0	1	0
0	1	1	0
1	1	0	1

Compound **2** with one fluorophore and two receptors can be stepwise protonated, because the two receptors have significantly different pK_a values, 7.78 for *N*-benzoylpiperazine and 4.60 for 8-methylquinoline as models.[23] As discussed above, the fluorescence quantum yield of compound **2** is around 0.017. When one equivalent of strong trifluoromethanesulfonic acid (CF_3SO_3H) is added, a fluorescence enhancement of the 4-amino-1,8-naphthalimide chromophore (Φ_f = 0.67 for **2H$^+$**) results. This fluorescence enhancement is due to blocking of PET.[24,25] Further protonation of the quinolinyl residue with a second equivalent of CF_3SO_3H leads to a pronounced quenching of fluorescence intensity (ca. 98% quenching) due to the formation of the quinolinium cation. Is assumed that the hydrogen-bonding of the quinolinium NH^+ with the imide carbonyl (C=O) is at the origin of the fluorescence quenching of the 4-amino-1,8-naphthalimide derivative (Scheme 3.3).[24] In essence an *off-on-off* fluorescence switch is obtained; see also Figure 3.2 and 3.3.

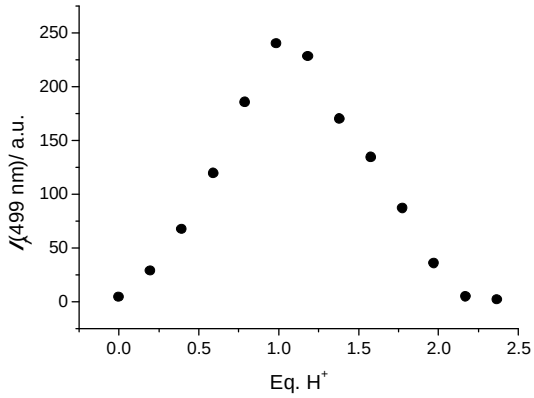

Figure 3.2. Fluorescence titration curve (λ_{exc} = 388 nm, λ_{obs} = 499 nm) of **2** (12.5 µM in acetonitrile) upon CF_3SO_3H addition.

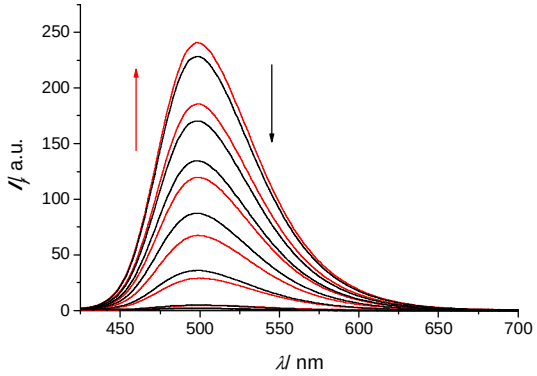

Figure 3.3. Fluorescence spectra (λ_{exc} = 388 nm) of **2** (12.5 µM in acetonitrile) upon titration with CF_3SO_3H. The red spectra correspond to 0-1 equiv. acid and the black spectra to 1.2-2.6 equiv. acid.

Hence, in accordance with the truth table of a T-latch (Table 3.2), the fluorescence signal is low (binary 0) in the absence of inputs, high (binary 1) for the addition of acid input in case of $Q_{current}$ = 0 (**2**→**2H**$^+$), and again low for another acid input addition in case of $Q_{current}$ = 1 (**2H**$^+$→**2H$_2$**$^{2+}$). The absence of acid leads to the hold situation ($Q_{current}$ = Q_{next}).

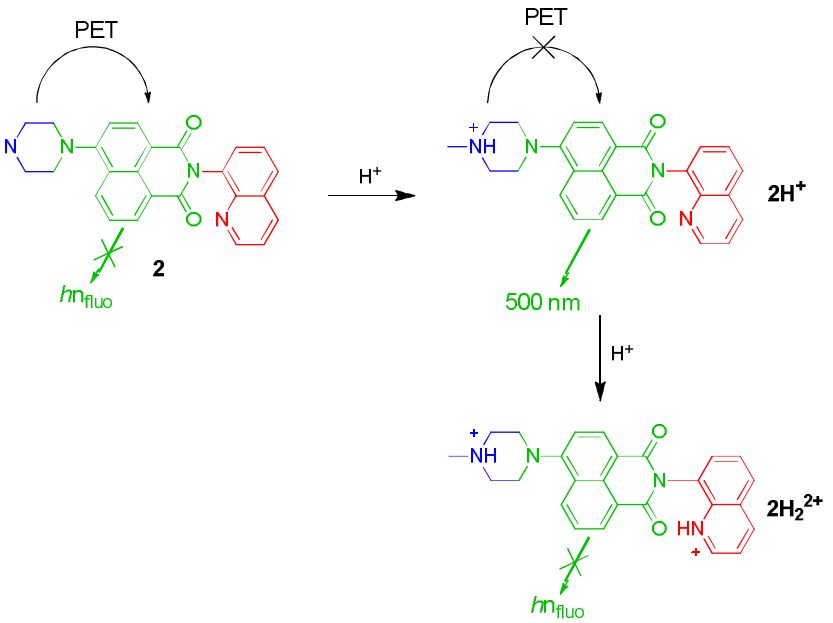

Scheme 3.3. Fluorescence switching of **2** upon addition of protons.

By observation of the photophysical effects upon protonation of the two models (compounds **3** and **5**) and by comparing them with the corresponding processes of compound **2**, it is possible to demonstrate the independent actuation of the two receptors. The protonation of the quinolinyl residue of the compound **3** leads to a quenching of the emission fluorescence (Figure 3.4 and 3.5).

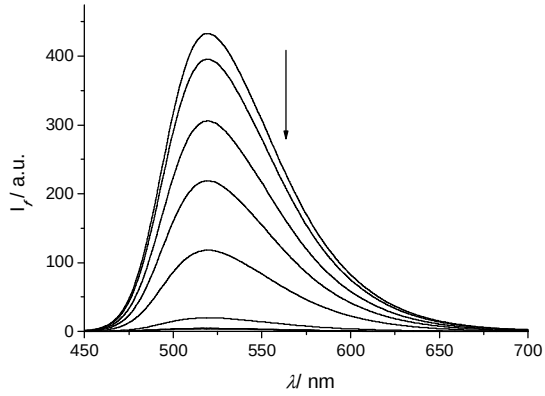

Figure 3.4. Fluorescence spectra (λ_{exc} = 432 nm) of **3** (14.2 µM in acetonitrile) upon titration with CF_3SO_3H.

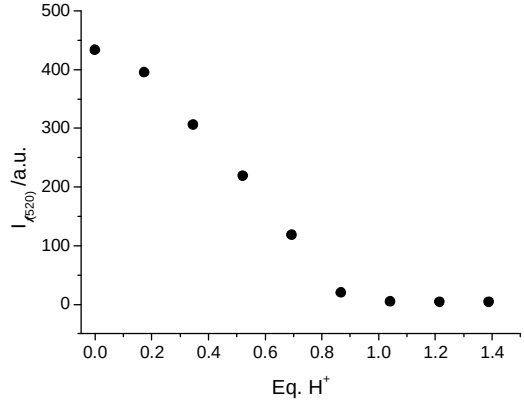

Figure 3.5. Fluorescence titration curve (λ_{exc} = 432 nm; λ_{obs} = 520 nm) of compound **3**.

For compound **5**, with the piperazinyl moiety as receptor, there is an enhancement of fluorescence when one equivalent of protons is added (Figure 3.6 and 3.7).

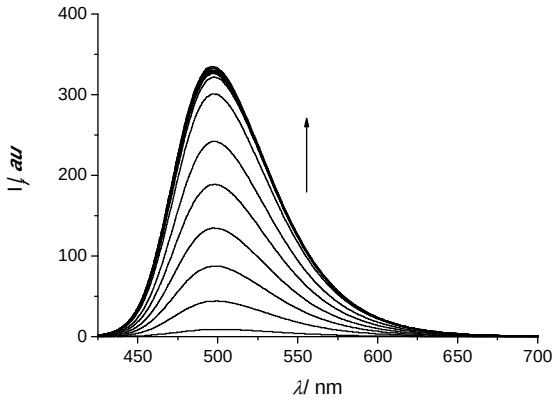

Figure 3.6. Fluorescence spectra (λ_{exc} = 386 nm) of **5** (9.2 µM in acetonitrile) upon titration with CF_3SO_3H.

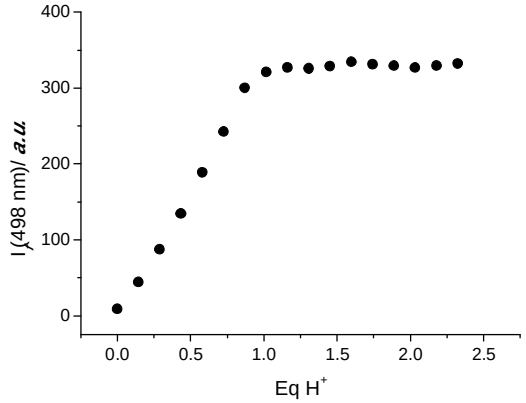

Figure 3.7. Fluorescence titration curve (λ_{exc} = 386 nm; λ_{obs} = 498 nm) of compound **5**.

The T-latch requires that the system must have a possibility to be reset after its final state ($\mathbf{2H_2^{2+}}$) has been reached, because the addition of another equivalent of acid would be without further effect. Resetting of the system can be easily achieved by application of a strong base (P_2-Et phosphazene) leading the inverse titration curve. The system can be reset for at least five cycles without much loss of the dynamic fluorescence switching range (see Appendix A).

Another condition to implement a correctly working T-latch is that the output $Q_{current}$= 0 for the two situations **2** and $\mathbf{2H_2^{2+}}$ must be distinguishable. This can be resolved by reading a control channel.[17,26-28] By observation of the absorption titration spectra of the second protonation ($\mathbf{2H^+ \rightarrow 2H_2^{2+}}$) corresponding to the protonation of the quinoline unit, a new band at 313 nm becomes notable (Figure 3.8).

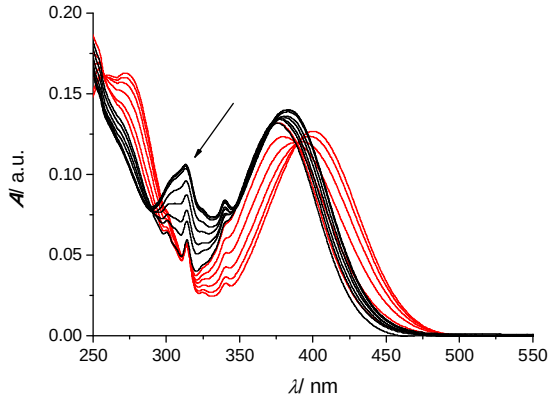

Figure 3.8. Absorption spectra of **2** (12.5 µM in acetonitrile) upon titration with CF_3SO_3H. The red spectra correspond to 0-1 equiv. acid and the black spectra to 1.2-2.6 equiv. acid.

Hence, when the fluorescence is low and the absorbance at 313 nm is high, two equivalents of base are needed to reset the system to the initial, unprotonated state corresponding to **2** (Table 3., 4th column of the truth table).[29] On the other hand, if the fluorescence and absorbance at 313 nm are both low, the system is already in its initial state. Hence, by reading the control channel the two $Q_{current}$ = 0 situations are perfectly differentiable.

3.5 Conclusion

In detail, it was shown that the fluorescence of the aminonaphthalimide-containing compound **2** can be switched by addition of chemical inputs (protons). In the absence of input application the system has a low fluorescence due to excited state quenching by PET. However, the addition of one equivalent of protons yields fluorescence enhancement due to the blocking of PET from an electron-donating piperazinyl unit. Further addition of a second equivalent of acid leads again to a pronounced drop in emission, which is reasoned with the protonation of the quinolinyl unit and a possible hydrogen bonding interaction of the NH^+ with the imide C=O. In brief, an *off-on-off* fluorescent switch results. Additionally, the molecule gives a differentiated fluorescence output that depends on the current state. The binary logic behaviour of the molecular system is compatible with that of a T-latch.

3.6 References

[1] Pischel, U. *Angew. Chem. Int. Ed.* **2007**, *46*, 4026.

[2] Andréasson, J.; Pischel, U. *Chem. Soc. Rev.* **2010**, *39*, 174.

[3] Pischel, U. *Aust. J. Chem.* **2010**, *63*, 148.

[4] Konry, T.; Walt, D. R. *J. Am. Chem. Soc.* **2009**, *131*, 13232.

[5] Margulies, D.; Hamilton, A. D. *J. Am. Chem. Soc.* **2009**, *131*, 9142.

[6] Privman, M.; Tam, T. K.; Bocharova, V.; Halámek, J.; Wang, J.; Katz, E. *ACS Appl. Mater. Interfaces* **2011**, *3*, 1620.

[7] Amir, R. J.; Popkov, M.; Lerner, R. A.; Barbas III, C. F.; Shabat, D. *Angew. Chem. Int. Ed.* **2005**, *44*, 4378.

[8] Ozlem, S.; Akkaya, E. U. *J. Am. Chem. Soc.* **2009**, *131*, 48.

[9] Hammarson, M.; Andersson, J.; Li, S.; Lincoln, P.; Andréasson, J. *Chem. Commun.* **2010**, *46*, 7130.

[10] Motornov, M.; Zhou, J.; Pita, M.; Gopishetty, V.; Tokarev, I.; Katz, E.; Minko, S. *Nano Lett.* **2008**, *8*, 2993.

[11] Angelos, S.; Yang, Y. W.; Khashab, N. M.; Stoddart, J. F.; Zink, J. I. *J. Am. Chem. Soc.* **2009**, *131*, 11344.

[12] Tokarev, I.; Gopishetty, V.; Zhou, J.; Pita, M.; Motornov, M.; Katz, E.; Minko, S. *ACS Appl. Mater. Interfaces* **2009**, *1*, 532.

[13] Margulies, D.; Melman, G.; Shanzer, A. *J. Am. Chem. Soc.* **2006**, *128*, 4865.

[14] Amelia, M.; Baroncini, M.; Credi, A. *Angew. Chem. Int. Ed.* **2008**, *47*, 6240.

[15] Pérez-Inestrosa, E.; Montenegro, J.-M.; Collado, D.; Suau, R. *Chem. Commun.* **2008**, 1085.

[16] Ceroni, P.; Bergamini, G.; Balzani, V. *Angew. Chem. Int. Ed.* **2009**, *48*, 8516.

[17] Andréasson, J.; Pischel, U.; Straight, S. D.; Moore, T. A.; Moore, A. L.; Gust, D. *J. Am. Chem. Soc.* **2011**, *133*, 11641.

[18] de Silva, A. P.; Goligher, A.; Gunaratne, H. Q. N.; Rice, T. E. *Arkivoc* **2003**, 229.

[19] Szaciłowski, K. *Chem. Rev.* **2008**, *108*, 3481.

[20] de Silva, A. P.; Gunaratne, H. Q. N.; Gunnlaugsson, T.; Huxley, A. J. M.; McCoy, C. P.; Rademacher, J. T.; Rice, T. E. *Chem. Rev.* **1997**, *97*, 1515.

[21] de Silva, A. P.; Vance, T. P.; West, M. E. S.; Wright, G. D. *Org. Biomol. Chem.* **2008**, *6*, 2468.

[22] Duke, R. M.; Veale, E. B.; Pfeffer, F. M.; Kruger, P. E.; Gunnlaugsson, T. *Chem. Soc. Rev.* **2010**, *39*, 3936.

[23] The pK_a data were taken from http://research.chem.psu.edu/brpgroup/pKa_compilation.pdf.

[24] de Silva, A. P.; Gunaratne, H. Q. N.; Habib-Jiwan, J.-L.; McCoy, C. P.; Rice, T. E.; Soumillion, J.-P. *Angew. Chem. Int. Ed. Engl.* **1995**, *34*, 1728.

[25] Tian, H.; Xu, T.; Zhao, Y.; Chen, K. *J. Chem. Soc., Perkin Trans. 2* **1999**, 545.

[26] Remón, P.; Hammarson, M.; Li, S.; Kahnt, A.; Pischel, U.; Andréasson, J. *Chem. Eur. J.* **2011**, *17*, 6492.

[27] Remón, P.; Ferreira, R.; Montenegro, J.-M.; Suau, R.; Pérez-Inestrosa, E.; Pischel, U. *ChemPhysChem* **2009**, *10*, 2004.

[28] Semeraro, M.; Credi, A. *J. Phys. Chem. C* **2010**, *114*, 3209.

[29] Schulman, S. G.; Capomacchia, A. C. *J. Am. Chem. Soc.* **1973**, *95*, 2763.

Chapter 4

Borylated Arylisoquinolines as Tunable Internal-Charge-Transfer Fluorophores

4. Borylated Arylisoquinolines as Tunable Internal-Charge-Transfer Fluorophores

This chapter is related to the manuscript:

> ***Borylated Arylisoquinolines: Photophysical Properties and Switching Behavior of Promising Tunable Fluorophores***
>
> Pais, V. F.; El-Sheshtawy, H. S.; Fernández, R.; Lassaletta, J. M.; Ros, A.; Pischel, U. *Chem. Eur. J.* **2013**, *19*, 6650-6661.

4.1 Introduction

The synthesis and characterization of organoboron compounds has been a challenge for researchers due to their interesting photophysical properties and multiple applications as luminescent polymeric materials,[1-6] in nonlinear optics,[7,8] as model chromophores for the study of electron transfer,[9,10] and as chemosensors for anions.[11-14]

The trigonal planar structure of trisubstituted organoboron compounds, where the boron features a sp^2 hybridization and a vacant p_π orbital, makes them susceptible to coordination with Lewis bases (such as F^- anions) and for charge-transfer phenomena. The Lewis acid-base interaction with the boron is often accompanied by *on-off*[15,16] or *off-on* fluorescence switching,[17-19] or even a ratiometric emission response.[7,20-27] Hence, it is possible to change the photophysical properties of these compounds by addition of anions leading to applications as chromogenic or fluorescent sensors.

In this chapter, a series of nine borylated arylisoquinolines with electronically tunable internal-charge-transfer (ICT) fluorescence emission

in an ample spectral window will be discussed. The fluorescence can be tuned by the electronic properties of the aryl moiety, by protonation of the isoquinoline group with acid (H^+) or by formation of fluoroboronate complexes with F^- anions.[28-30]

4.2 Molecular Design

The borylated arylisoquinolines are designed based on three criteria (Scheme 4.1):

- Existence of a site for coordination of fluoride (F^-) ions;
- Existence of a site for protonation with trifluoroacetic acid (TFA);
- Possibility of the observation of ICT.

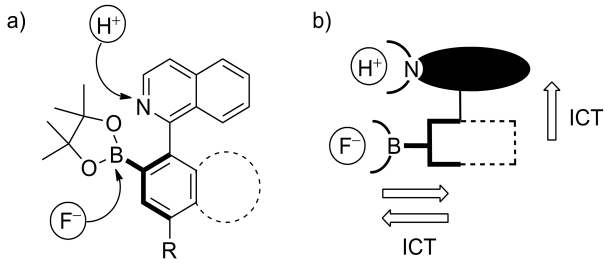

Scheme 4.1. Molecular design of dually switchable borylated arylisoquinolines. a) General structure and indication of binding sites. b) Schematic representation of possible ICT interactions.

Taking into account these preconditions a series of borylated arylisoquinolines with different aryl moieties (comprising naphthyl, acenaphthyl, pyrenyl and anthryl) was synthesized. In the case of the naphthyl moieties the substitution with electron-withdrawing or electron-donating groups was also varied. The corresponding non-borylated analogues serve as photophysical model compounds (Scheme 4.2).

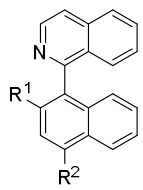

R^1= Bpin; R^2=H; **1**
R^1= Bpin; R^2=CN; **2**
R^1= Bpin; R^2=F; **3**
R^1= Bpin; R^2=CH_3; **4**
R^1= Bpin; R^2=OCH_3; **5**
R^1= Bpin; R^2=$N(CH_3)_2$; **6**

R^1, R^2=H; **M1**
R^1= H; R^2=CN; **M2**
R^1= H; R^2=F; **M3**
R^1= H; R^2=CH_3; **M4**
R^1= H; R^2=OCH_3; **M5**
R^1= H; R^2=$N(CH_3)_2$; **M6**

Bpin: 

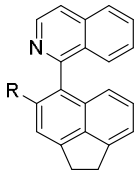

R = Bpin; **7**
R = H; **M7**

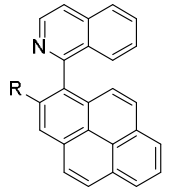

R = Bpin; **8**
R = H; **M8**

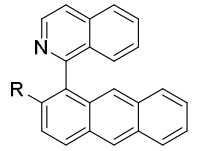

R = Bpin; **9**
R = H; **M9**

Scheme 4.2. Structures of the borylated arylisoquinolines **1**-**9** and their respective models **M1**-**M9**. The numbering of the compounds corresponds to the related manuscript (see Appendix B).

4.3 Photophysical Properties

All photophysical key data of the compounds **1**-**9** are summarized in Table 4.1. The UV/vis bands are in the region of 250-400 nm and the fluorescence spectra show a dominant broad and red-shifted long-wavelength (LW) emission band that is often accompanied by a weaker and blue-shifted short-wavelength (SW) emission. An exception is compound **2** with a cyano (CN) group, which has only one emission band.

Table 4.1. UV/vis absorption and fluorescence properties of borylated arylisoquinolines **1**-**9** in acetonitrile.

	$\lambda_{abs,\,max}$/ nm	ε/ $M^{-1}cm^{-1}$	$\lambda_{fluo,\,max}$/ nm	Φ_f[b]	I_{fl}(LW)/I_{fl}(SW)	τ_f/ns (%)[c]
1	284	9500	368, 492	0.01	3	0.32 (98.3)
2	309	10200	437	0.01	-[d]	0.26 (98.1)
3	286	8250	362, 494	0.02	21	1.00 (91.8)
4	287	9700	386, 502	0.04	25	2.51 (98.5)
5	309	9100	424, 532	0.43	123	7.81 (81.2)
6	323	6200	420, 608	0.36	149	6.11 (100)
7	291	8300	417, 527	0.20	41	7.95 (100)
8	341	33000	391, 412, 528	0.27	29	3.32 (100)
9	371	4800	428, 571	0.1	6	3.28 (100)

[a] Value refers to λ_{abs}. [b] Total fluorescence quantum yield. [c] Fluorescence lifetime of the main component (weight is given in parentheses). [d] Only one fluorescence band is observed.

The maximum of the LW emission band can be correlated with the oxidation potential of the aryl moiety (see Figure 4.1).[31,32] This is in agreement with the involvement of ICT processes in the emission of the dyes.

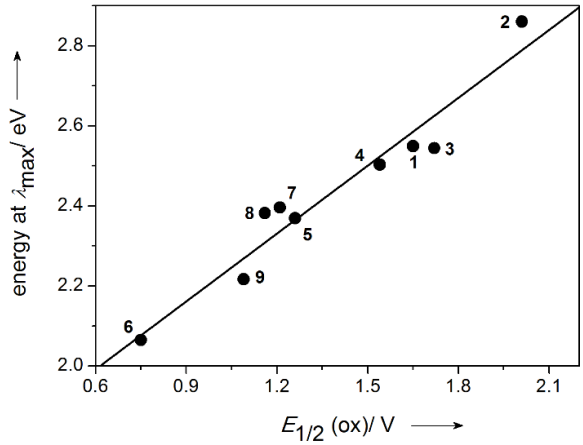

Figure 4.1. Linear plot of the energy corresponding to the principal fluorescence emission maximum versus the half-wave oxidation potential of the aryl moiety.

Observing the graph shown in Figure 4.1 it is possible to conclude that compound **6**, which has the easiest to oxidize aryl residue ($E_{1/2}$(ox)= 0.75 V versus SCE in acetonitrile),[31] shows the most red-shifted band (λ_{max}= 608 nm). On the other hand, compound **2** with the most difficult to oxidize aryl residue ($E_{1/2}$(ox)= 2.01 V versus SCE in acetonitrile)[32] shows the most blue-shifted emission band in the series. Hence, it can be assumed that ICT is a decisive factor for the photophysical behavior of the borylated arylisoquinolines. This is in some analogy to biaryl systems that show dual fluorescence and where the SW band can be assigned to a locally-excited (LE) state while the LW band corresponds to an ICT state.[33] This assignment to an ICT state is further corroborated by observing solvatochromic effects.[34] The SW band shows no significant spectral shift upon changing the solvent medium, but the ratio I_{fl}(LW)/I_{fl}(SW) decreases in solvents of lower polarity. This is in agreement with the made assignments because a lower solvent polarity would destabilize the ICT state, and thus, emission from the LE state gains more weight. The LW band of the compounds with most significant ICT character (**6**, **8**, **9**) shows the largest bathochromic shifts upon changing from non-polar toluene to polar acetonitrile. For the other compounds (**1**-**5** and **7**) the effects are

smaller or even negligible (the case of compound **2**, see Table 4.2). The plot of the LW fluorescence maximum versus Reichardt's $E_T(30)$[35] parameter confirms the significantly higher ICT character for the dyes with strong electron-donating aryl residues (see Appendix B).

Concerning the emission quantum yields, for compounds with weak ICT character (more positive aryl oxidation potentials) lower values are observed. On the other hand, for compound **5**, that contains the electron-donating methoxy group, a fluorescence quantum as high as 0.43 is measured. Compound **6**, with the most pronounced ICT character in the investigated series, shows a small drop in the emission quantum yield (Φ_f = 0.36). This behavior is explained by invoking the energy-gap law: the lower-lying the emissive state, the more competitive are non-radiative deactivation processes. The same trend is observed for the compounds **1**, **7**, **8**, **9**, a small sub-series where the degree of π-conjugation of the aryl residue is varied.

For the non-borylated compounds **M1**-**M9** no significant differences in the UV/vis spectra in comparison to the borylated derivatives are noted. However, in the fluorescence spectra only one weak emission band is observed. This band normally appears near the position of the SW band of the borylated derivatives (when observed). The emission quantum yield is generally low for the non-borylated models (< 0.01). This underlines the importance of the boron-substituent for the observation of strong and red-shifted emission of the borylated arylisoquinolines (see Appendix B).

Table 4.2. Redox potentials, solvatochromic effects, fluoride binding constants for the compounds **1**-**9**, and their fluorescence modulation upon addition of trifluoroacetic acid (TFA) or tetra-*n*-butylammonium fluoride (Bu_4NF).

	E_{ox}/V [a]	$\Delta\lambda$/ nm [b]	K/ M^{-1} [c]	Q in % [d] (TFA)	Q in % [d] (Bu_4NF)
1	1.65 [e]	1	$(6.9\pm0.6) \times 10^3$	[f]	70
2	2.01 [e]	-2	$>10^6$ [g]	[f]	93
3	1.72 [e]	3	$(6.9\pm0.9) \times 10^4$	5	85
4	1.54 [e]	5	$(3.7\pm0.1) \times 10^3$	59	89
5	1.26 [e]	11	$(2.1\pm0.1) \times 10^4$	96	96
6	0.75 [h]	26	$(9.5\pm0.3) \times 10^3$	99	96
7	1.21 [e]	15	$(3.3\pm0.6) \times 10^3$	87	78
8	1.16 [n]	19	$(1.9\pm0.1) \times 10^4$	91	86
9	1.09 [n]	27	$(1.4\pm0.2) \times 10^4$	96	98

[a] Half-wave oxidation potential of aryl models (*versus* SCE in MeCN): **1**: naphthalene, **2**: 1-cyanonaphthalene, **3**: 1-fluoronaphthalene, **4**: 1-methylnaphthalene, **5**: 1-methoxynaphthalene, **6**: 1-(*N*,*N*-dimethylamino)naphthalene, **7**: acenaphthene, **8**: pyrene, **9**: anthracene. [b] Solvatochromic shift of the LW fluorescence maximum upon changing from toluene to acetonitrile. [c] 1:1 Binding constant of fluoride resulting in a fluoroboronate complex; measured by fluorescence titration. [d] Fluorescence quenching of the LW emission band (measured at the maximum wavelength) upon addition of 10 equiv TFA or 60 equiv Bu_4NF. [e] See ref. 32. [f] Fluorescence enhancement is observed: factor of 3.6 and 4.3 for **1** and **2**, respectively. [g] Lower limit, too large to be measured accurately. [h] See ref. 31.

4.4 Density-Functional-Theory Calculations

To corroborate the experimental observations, density-functional-theory (DFT) calculations were realized for the compounds **1**-**6**. Contour plots of the frontier orbitals of the optimized structures [B3LYP/6-31+G(d,p) level of theory] of the compounds **2**, **4**, and **6** are presented in Figure 4.2.

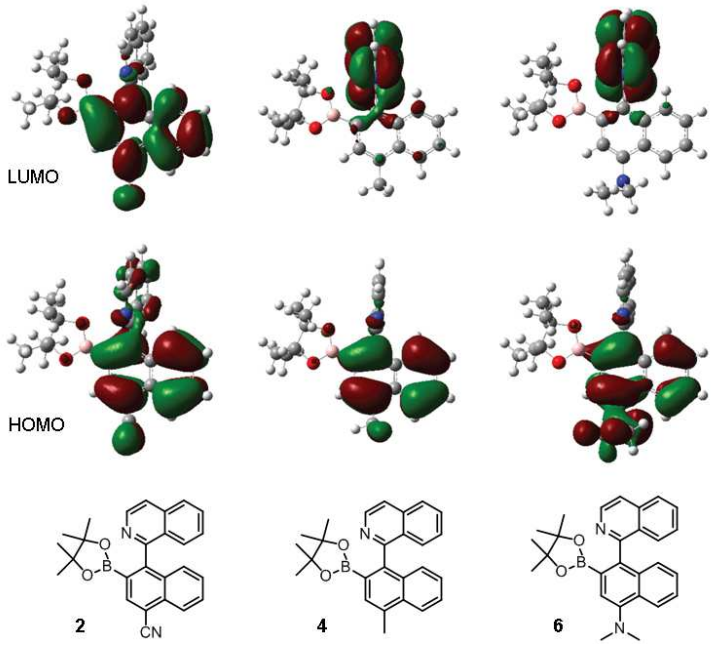

Figure 4.2. HOMO and LUMO contour plots of the optimized molecular geometries [B3LYP/6-31+G(d,p) level of theory] of the compounds **2**, **4**, and **6**.

By observing Figure 4.2 it is easily confirmed that for dyes with electron-donor aryl moieties the HOMO (highest occupied molecular orbital) orbital is localized on the borylated aryl residue and that the LUMO (lowest unoccupied molecular orbital) is situated on the isoquinolinyl group. This suggests that the aryl moiety is involved as a donor and the isoquinolinyl group as an acceptor in the ICT process. On the other hand, for compound **2**, the HOMO and the LUMO are located on the borylated aryl residue, in agreement with the assignment of an LE state as the lowest-energy transition.

By observing the HOMO energies (see Appendix B), it is possible to conclude that compound **2** has the lowest-lying HOMO, because the aryl residue is the most difficult one to oxidize in the investigated series. On the other hand, compound **6**, featuring the strong electron-donating $N(CH_3)_2$ group, features the highest-lying HOMO.

4.5 Addition of Protons

In the case of borylated compounds, the fluorescence response upon addition of 10 equivalents of TFA is dependent on the electronic conditions of the system. For compounds with aryl residues with weak donor/acceptor character (**1** and **3**) or strong electron-accepting properties (**2**) fluorescence enhancement or only a minor quenching effect (for **3**) are observed (see Table 4.2). The protonation of the isoquinoline groups leads to the formation of an electron-accepting isoquinolinium cation and consequently to an increased degree of ICT that is accompanied by a fluorescence enhancement.

The other compounds give moderate fluorescence quenching (up to 59%) of the LW band. For compounds with pronounced ICT character (**5**-**9**) the formation of the isoquinolinium cation and an additional stabilization of the ICT state favors their preferential deactivation through non-radiative processes (energy-gap law).

For the non-borylated arylisoquinolines the addition of acid produces red-shifted LW emission bands that appear at similar positions as the ones observed for the borylated derivatives. This behavior is assigned to the formation of an ICT state, which is supported by appearance of new red-shifted UV/vis absorption bands ($\Delta\lambda$ = 330-450 nm). For the compounds **M6** and **M9**, the addition of protons shows fluorescence quenching.

The fluorescence response with metal cations such as Na^+, Ag^+, Mg^{2+}, Pb^{2+} and Zn^{2+} was also studied. When Na^+ is used no fluorescence modulation is observed. For Pb^{2+} and Zn^{2+}, in case of compounds **6** and **9**, a strong quenching results due to a heavy-atom-induced intersystem crossing (Pb^{2+}) or redox quenching (Zn^{2+}). However, because of the capacity of the hydrated heavy metal ions to act as Brønsted acids, the protonation of the isoquinoline could also be responsible for the observed quenching effects.

4.6 Addition of Anions

It is well-known that fluoride ions (F^-) form Lewis acid-base adducts with boron-substituted fluorophores.[36] The herein investigated dyes **1**-**9** are no exception in this respect. For all compounds a strong fluorescence quenching is observed upon addition of F^-. The formation of the F^- adduct turns the boronic ester into a fluoroboronate substituent,[37] which is known as one of the strongest inductively donating groups.[13] Hence, this increased electron-donating propensity of the aromatic moiety leads to an energetically lower-lying ICT state and concomitant fluorescence quenching according to the energy-gap law. By following the fluorescence as a function of the added F^- concentration, the 1:1 F^- binding constants by the boronic acid esters are determined (see Table 4.2).

For the compounds **2** and **3** the binding constants are high, owing to the electron-deficient nature of the aryl residue. The CN and F substituents are electron-withdrawing and apparently increase the Lewis acidity of the boron center.[38,39] All other compounds have binding constants between 3×10^3 and 2×10^4 M^{-1}. To prove the formation of the Lewis adduct, the corresponding complex was detected for the example of compound **9** by electrospray ionization mass spectrometry. The spectrum shows clearly a peak at *m*/*z* = 450 which is assigned to **9F**$^-$. The same conclusion of Lewis adduct formation is reached from the results obtained by ^{11}B NMR spectroscopy. When 0.5 equivalents of Bu_4NF are added to a solution of compound **9**, the initial signal at δ = 31.1 ppm, corresponding to tri-coordinated boron in the boronic acid ester, decreases and finally disappears upon addition of 1.0 equivalent of Bu_4NF. Concomitantly the typical ^{11}B NMR resonance of the tetra-ccoordinated boron in the fluoroboronate complex at δ = 7.0 ppm is observed as new signal.[40]

Interestingly, compound **9** showed ratiometric fluorescence behavior where the LW emission band at 571 nm was quenched and concomitantly a blue shifted band at *ca*. 420 nm was formed (see Appendix B).[7,20-27] By

observing the DFT calculations it is possible to see that the HOMO is located on the anthryl group and the LUMO involves the anthryl-boron pinacolate moiety. This hints on a charge transfer from the aryl moiety to the boronic acid ester substituent. The F^- coordination blocks this process and a blue-shifted emission from an LE state is observed. With other anions (Cl^-, Br^-, CN^-, NO_3^-, CH_3COO^-, and $H_2PO_4^-$) no fluorescence alterations are notable. The only exception is compound **2**, which shows some fluorescence quenching with CN^- and $H_2PO_4^-$ (see Appendix B1).

4.7 Conclusion

In conclusion, nine borylated compounds were tested as potential molecular fluorescence switches. The fluorescence properties of the compounds are based on ICT processes, where the boronic acid ester substituent plays an important role. Compounds that contain weakly electron-donating aryl moieties show a blue-shifted emission while compounds with easy to oxidize aryl residues show LW emission in the red-shifted spectral region. The ICT phenomena are further corroborated by the observation of significant solvatochromic effects and have been characterized by density-functional-theory calculations. The latter corroborate the involvement of the aryl moiety (HOMO) and the isoquinolinyl residue (LUMO) in the charge transfer.

The emission properties are changed by addition of external chemical stimuli such as protons and fluoride ions. The protonation of the isoquinoline moiety by addition of acid leads to fluorescence enhancement for compounds that show weak charge transfer and fluorescence quenching for compounds that show stronger charge transfer. The addition of fluoride ions quenches the fluorescence due to the formation of fluoroboronate complexes involving the boron-pinacolate moiety.

The borylated arylisoquinolines have potential applications for fluoride sensing in non-aqueous media or as pH-dependent fluorescent tags with tunable emission color.

4.8 References

[1] Entwistle, C. D.; Marder, T. B. *Angew. Chem. Int. Ed.* **2002**, *41*, 2927.

[2] Entwistle, C. D.; Marder, T. B. *Chem. Mater.* **2004**, *16*, 4574.

[3] Parab, K.; Venkatasubbaiah, K.; Jäkle, F. *J. Am. Chem. Soc.* **2006**, *128*, 12879.

[4] Qin, Y.; Kiburu, I.; Shah, S.; Jäkle, F. *Macromolecules* **2006**, *39*, 9041.

[5] Elbing, M.; Bazan, G. C. *Angew. Chem. Int. Ed.* **2008**, *47*, 834.

[6] Li, H.; Jäkle, F. *Angew. Chem. Int. Ed.* **2009**, *48*, 2313.

[7] Liu, Z.-Q.; Shi, M.; Li, F.-Y.; Fang, Q.; Chen, Z.-H.; Yi, T.; Huang, C.-H. *Org. Lett.* **2005**, *7*, 5481.

[8] Collings, J. C.; Poon, S.-Y.; Le Droumaguet, C.; Charlot, M.; Katan, C.; Pålsson, L.-O.; Beeby, A.; Mosely, J. A.; Kaiser, H. M.; Kaufmann, D.; Wong, W.-Y.; Blanchard-Desce, M.; Marder, T. B. *Chem. Eur. J.* **2009**, *15*, 198.

[9] Stahl, R.; Lambert, C.; Kaiser, C.; Wortmann, R.; Jakober, R. *Chem. Eur. J.* **2006**, *12*, 2358.

[10] Schmidt, H. C.; Reuter, L. G.; Hamacek, J.; Wenger, O. S. *J. Org. Chem.* **2011**, *76*, 9081.

[11] Hudnall, T. W.; Chiu, C.-W.; Gabbaï, F. P. *Acc. Chem. Res.* **2009**, *42*, 388.

[12] Hudson, Z. M.; Wang, S. *Acc. Chem. Res.* **2009**, *42*, 1584.

[13] Wade, C. R.; Broomsgrove, A. E. J.; Aldridge, S.; Gabbaï, F. P. *Chem. Rev.* **2010**, *110*, 3958.

[14] Guo, Z.; Shin, I.; Yoon, J. *Chem. Commun.* **2012**, *48*, 5956.

[15] Hudnall, T. W.; Gabbaï, F. P. *J. Am. Chem. Soc.* **2007**, *129*, 11978.

[16] Lee, M. H.; Agou, T.; Kobayashi, J.; Kawashima, T.; Gabbaï, F. P. *Chem. Commun.* **2007**, 1133.

[17] Kubo, Y.; Kobayashi, A.; Ishida, T.; Misawa, Y.; James, T. D. *Chem. Commun.* **2005**, 2846.

[18] Swamy, K. M. K.; Lee, Y. J.; Lee, H. N.; Chun, J.; Kim, Y.; Kim, S.-J.; Yoon, J. *J. Org. Chem.* **2006**, *71*, 8626.

[19] Zhou, G.; Baumgarten, M.; Müllen, K. *J. Am. Chem. Soc.* **2008**, *130*, 12477.

[20] Yamaguchi, S.; Shirasaka, T.; Akiyama, S.; Tamao, K. *J. Am. Chem. Soc.* **2002**, *124*, 8816.

[21] Kubo, Y.; Yamamoto, M.; Ikeda, M.; Takeuchi, M.; Shinkai, S.; Yamaguchi, S.; Tamao, K. *Angew. Chem. Int. Ed.* **2003**, *42*, 2036.

[22] Liu, X. Y.; Bai, D. R.; Wang, S. *Angew. Chem. Int. Ed.* **2006**, *45*, 5475.

[23] Bai, D.-R.; Liu, X.-Y.; Wang, S. *Chem. Eur. J.* **2007**, *13*, 5713.

[24] Yuan, M.-S.; Liu, Z.-Q.; Fang, Q. *J. Org. Chem.* **2007**, *72*, 7915.

[25] Sun, Y.; Wang, S. *Inorg. Chem.* **2009**, *48*, 3755.

[26] Xu, Z. C.; Kim, S. K.; Han, S. J.; Lee, C.; Kociok-Kohn, G.; James, T. D.; Yoon, J. *Eur. J. Org. Chem.* **2009**, 3058.

[27] Pan, H.; Fu, G.-L.; Zhao, Y.-H.; Zhao, C.-H. *Org. Lett.* **2011**, *13*, 4830.

[28] Kluciar, M.; Ferreira, R.; de Castro, B.; Pischel, U. *J. Org. Chem.* **2008**, *73*, 6079.

[29] Ferreira, R.; Remón, P.; Pischel, U. *J. Phys. Chem. C* **2009**, *113*, 5805.

[30] Remón, P.; Ferreira, R.; Montenegro, J.-M.; Suau, R.; Pérez-Inestrosa, E.; Pischel, U. *ChemPhysChem* **2009**, *10*, 2004.

[31] Montalti, M.; Credi, A.; Prodi, L.; Gandolfi, M. T. *Handbook of Photochemistry*; 3rd ed.; Taylor & Francis: Boca Raton, FL, **2006**.

[32] Abdel-Shafi, A. A.; Wilkinson, F. *Phys. Chem. Chem. Phys.* **2002**, *4*, 248.

[33] Grabowski, Z. R.; Rotkiewicz, K.; Rettig, W. *Chem. Rev.* **2003**, *103*, 3899.

[34] Suppan, P.; Ghoneim, N. *Solvatochromism*; The Royal Society of Chemistry: Cambridge, **1997**.

[35] Reichardt, C. *Solvents and Solvent Effects in Organic Chemistry*; 2nd ed.; VCH: Weinheim, **1990**.

[36] Bresner, C.; Day, J. K.; Coombs, N. D.; Fallis, I. A.; Aldridge, S.; Coles, S. J.; Hursthouse, M. B. *Dalton Trans.* **2006**, 3660.

[37] Galbraith, E.; James, T. D. *Chem. Soc. Rev.* **2010**, *39*, 3831.

[38] Yuchi, A.; Tatebe, A.; Kani, S.; James, T. D. *Bull. Chem. Soc. Jpn.* **2001**, *74*, 509.

[39] DiCesare, N.; Lakowicz, J. R. *J. Phys. Chem. A* **2001**, *105*, 6834.

[40] Nave, S.; Sonawane, R. P.; Elford, T. G.; Aggarwal, V. K. *J. Am. Chem. Soc.* **2010**, *132*, 17096.

Chapter 5

Borylated Arylisoquinolines as Fluorescent pH Switches for Multivalued Logic

5. Borylated Arylisoquinolines as Fluorescent pH Switches for Multivalued Logic

This chapter is related to the manuscript:

> ***Preparation and pH-Switching of Fluorescent Borylated Arylisoquinolines for Multilevel Molecular Logic***
>
> Pais, V. F.; Lineros, M.; López-Rodríguez, R.; El-Sheshtawy, H. S.; Fernández, R.; Lassaletta, J. M.; Ros, A.; Pischel, U. *J. Org. Chem.* **2013**, *78*, 7949-7961.

5.1 Introduction

Fluorescent compounds that work as molecular switches by the addition of chemical species are essential for areas such as analytical chemistry, environmental sciences, and clinical diagnostics.[1-5]

The measurement of pH by means of fluorescent probes is a simple but instructive example for the conceptual approach to fluorescence switching. The electronic structure of the switches determines the response to protonation, including fluorescence enhancement, quenching or both in form of a ratiometric answer. The fluorescence signals can be translated into binary notations by assigning a 0 or a 1 to the respective *off* or *on* states of the systems. This simple analogy enables the interpretation of such switches in terms of molecular information processing and logic.[6-12] Simple *on-off* (fluorescence quenching) or *off-on* switching (fluorescence enhancement) is relatively easy to implement with molecules. However, more complex situations such as *off-on-off* are

described less frequently and they are more challenging with regard to the involved molecular design.[12,13]

The combination of two antagonistic proton receptors with a fluorophore and photoinduced electron transfer (PET) as communication mechanism enables a general strategy for *off-on-off* and also *on-off-on* switches.[14-19] Normally, these switches use multi-level input signals (*low*, *medium*, or *high*) and their output is read through a binary low-high (0-1) convention. On the other hand, there are a few cases where fluorescent systems allow for the reading of three or even four stable output states leading to ternary or quaternary switching.[12,20]

The research reported in this chapter concerns the photophysical characterization of new pH-switchable fluorescent borylated arylisoquinoline dyes. These can be used as switches with *off-on-off* and *on-off-on'* character and they are also capable of generating ternary and quaternary outputs, thereby implementing multivalued logic.[12]

5.2 Molecular Design

The molecular design is based on the pH-switching of fluorescence. Accordingly four dyes (see Scheme 5.1) with two orthogonal proton receptor functions were investigated. The following structural features with regard to stepwise protonation were integrated:

- a tertiary amino function which has typically a pK_a of *ca*. 8-10 in water (e.g., pK_a *ca*. 8.4 for 1,4-dimethylpiperazine)[21]
- an isoquinoline moiety, with a much lower protonation constant (pK_a *ca*. 4.8 for parent isoquinoline in 1/1 methanol/water).[22] The two moieties have sufficiently different pK_a values so they can be protonated in an orthogonal manner.
- For one of the dyes it was also foreseen that the aromatic N could be protonated.

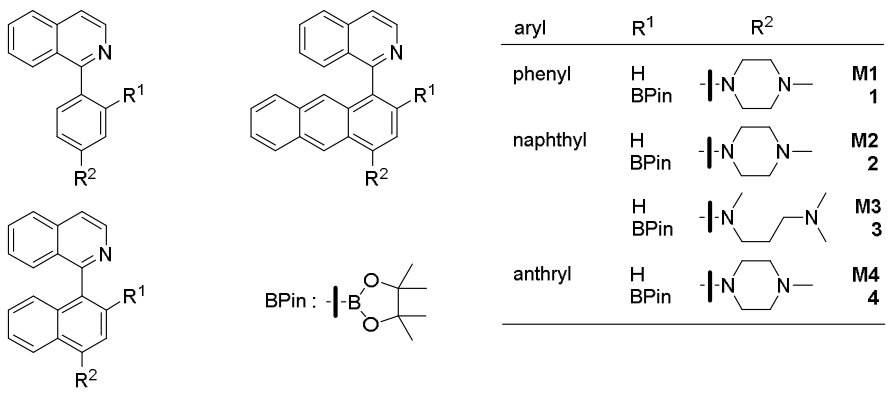

Scheme 5.1. Structures of the dyes **1**-**4** and their respective models **M1**-**M4**. The numbering refers to the article that corresponds to this chapter (see Appendix C).

The orthogonal protonation behavior can be investigated using spectroscopic techniques such as ^{1}H NMR. The ^{1}H NMR spectra for the example of dye **2** (Figure 5.1) show chemical shift alterations upon addition of acid (CF_3SO_3H). Upon the addition of one equivalent of acid the N-CH_3 (circle marks) methyl protons are downfield shifted ($\Delta\delta$ = +0.62 ppm), while the aromatic protons are much less affected. The addition of two equivalents of acid leads to changes in the aromatic region, which are due to the protonation of isoquinoline moiety. Observing the proton in *ortho* position (square marks) relative to the isoquinoline N, no signal change is seen for one equivalent of acid. However, with the addition of more acid (until two equivalents) a clear upfield shift and merging with other aromatic proton signals results.

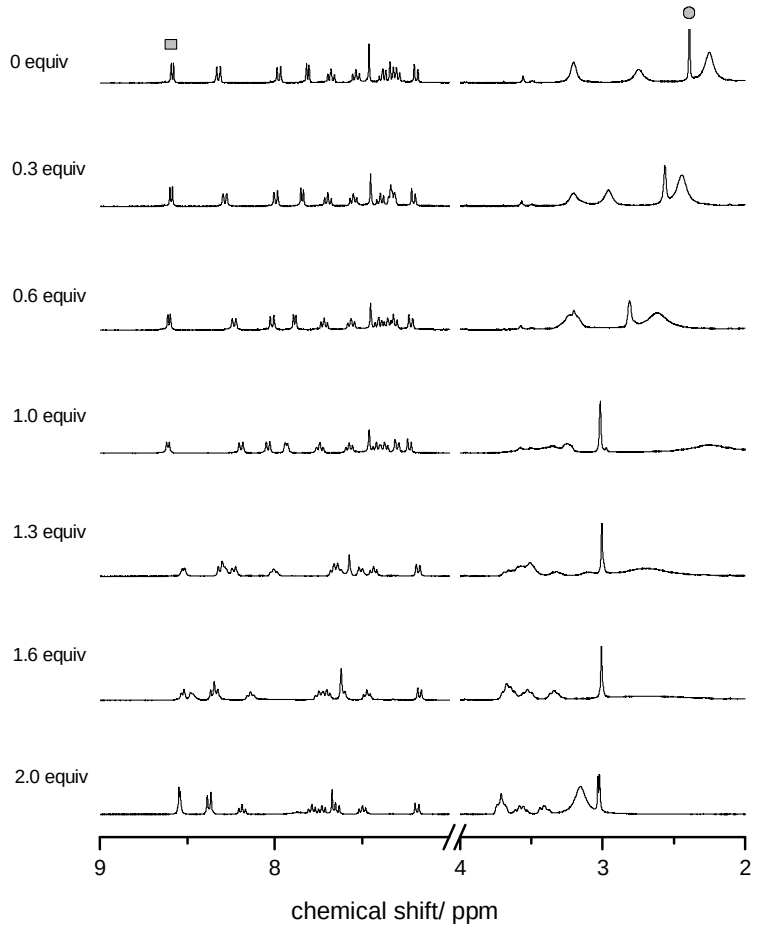

Figure 5.1. ^{1}H NMR spectra of dye **2** in acetonitrile-d_3 upon successive addition (0-2 equiv) of CF_3SO_3H. The square marks the proton in *ortho* position relative to the isoquinoline N, the circle marks the N-CH_3 protons of the piperazinyl unit.

The observations made for the ^{1}H NMR spectra are in agreement with the assumed orthogonal protonation behavior of the two receptors: the first equivalent of acid leads to the protonation at the lateral tertiary amino N, while the second acid equivalent protonates the isoquinoline N.

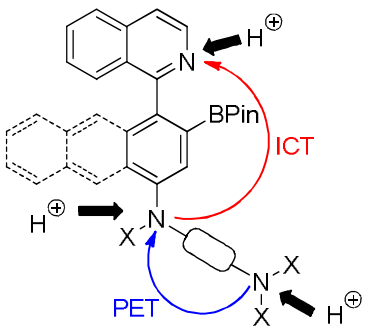

Scheme 5.2. Mechanistic proposal for excited state interactions and protonation sites of the dyes **1**-**4**.

As mentioned in Chapter 4 of this thesis, borylated arylisoquinolines show fluorescence that originates from an internal-charge-transfer (ICT) state. [23] The fluorescence can be influenced by protonation of the isoquinoline. In the present dyes there is an additional possibility of PET quenching. This pathway can be switched by protonation of the lateral amino function. These mechanistic possibilities and the corresponding protonation sites are generalized in Scheme 5.2.

5.3 Photophysical Characterization

All dyes were photophysically characterized in acetonitrile solution. The obtained UV/vis and fluorescence data are summarized in Table 5.. The UV/vis absorption and fluorescence spectra are shown in Figure 5.2.

Table 5.1. UV/vis absorption and fluorescence properties of borylated arylisoquinolines in acetonitrile.

	$\lambda_{abs,\ max}$/ nm	ε/ $M^{-1}cm^{-1}$ [a]	$\lambda_{f,\ max}$/ nm	Φ_f	τ_f/ ns [b]
1	420	12300	559	0.07	0.65 (82%), 6.64 (18%)
1H$^+$	400	10200	530	0.45	5.60
1H$_2^{2+}$	370	5300	537	0.01	1.15 (18%), 5.67 (82%)
2	323	9600	599	0.37	5.44
2H$^+$	311, 322	9800	576	0.50	7.09
2H$_2^{2+}$	327, 340	9800	[c]	[c]	[c]
3	323	7500	607	0.35	6.01
3H$^+$	323	8000	600	0.39	6.88
3H$_2^{2+}$	340	9100	[c]	[c]	[c]
3H$_3^{3+}$	333, 340	6400	447	0.03	1.24
4	388, 401	5400	526, 638	0.23	4.87
4H$^+$	380, 399	5400	502, 622	0.20	4.05
4H$_2^{2+}$	342, 388, 406	5900	502	0.01	11.00

[a] The molar absorption coefficient refers to the longest-wavelength absorption maximum. [b] The lifetime of the major component (≥ 95%) is shown, except for cases where two exponentials contributed significantly. [c] Non-fluorescent species.

Dye **1** has a broad absorption band at 420 nm. This band is more red-shifted than observed for the other dyes (**2**-**4**) that contain easier-to-oxidize aryl moieties. The formation of an intra-Lewis pair through the B-N interaction, visible in ^{11}B NMR (see Appendix C1), increases the electron density at the piperazinyl-phenyl moiety and as well turns the isoquinoline into a stronger electron acceptor unit. This rationalization is assumed to be the explanation for the observation of the ground-state charge-transfer (CT) band for dye **1**.

The UV/vis absorption bands for the dyes **2** and **3** (λ_{max} = 323 nm) are in the region that is typical for isoquinolines and substituted naphthalenes. Dye **4** features a band that is characteristic for an isoquinoline (λ_{max} = 321 nm) and a red-shifted band with two maxima at 388 and 401 nm, corresponding to the anthracene part.

The fluorescence spectra of all dyes show broad red-shifted bands with maxima between 560 nm (dye **1**) and 638 nm (dye **4**). The observation of the most red-shifted band for dye **4** is in accordance with the easily oxidizable piperazinyl-anthryl moiety (Figure 5.2).

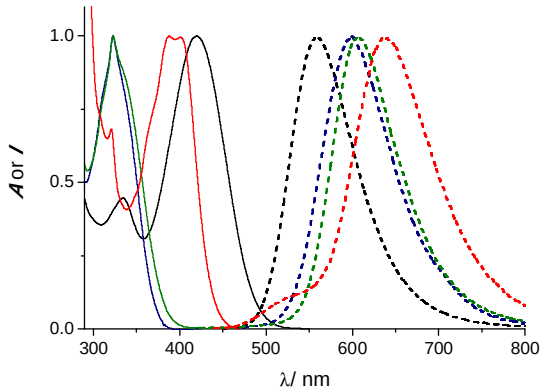

Figure 5.2. UV/vis absorption (solid lines) and fluorescence spectra (dashed lines) of the borylated arylisoquinoline dyes in acetonitrile; black: **1**, blue: **2**, green: **3**, red: **4**.

It is assumed that the small emission quantum yield of dye **1** (see Table 5.1) is due to the formation of the intra-Lewis pair (see above) and a reduced energy gap (note also the Stokes shift of only 140 nm for dye **1** *versus* 240–280 nm for the dyes **2**-**4**). This results in a low quantum yield as a consequence of highly competitive non-radiative pathways for excited-state deactivation (energy gap law). For the dyes **2**-**4** there is no B-N interaction and in these cases the quantum yield is between 0.23 and 0.37. The emission lifetimes, comparing dye **1** with the dyes **2**-**4**, showed similar trends.

For the non-borylated dyes **M2**-**M4** the UV/vis absorption bands are found in the same region as observed for the corresponding borylated analogues. However, for dye **M1** the spectrum shows a remarkable blue shift in comparison to dye **1**. This is reasoned with the absence of B-N interactions and lends indirect support to the charge transfer (CT) assignment to the long-wavelength absorption band of dye **1**. In the case of the fluorescence emission of the non-borylated model dyes all spectra are blue-shifted with respect to the borylated derivatives and reduced fluorescence quantum yields are obtained (see Appendix C1). This is in line with the general observation of the significant influence of the boronic acid ester substituent on the photophysical properties of the dyes (see also Chapter 4 for related observations).

5.4 Density-Functional-Theory Calculations

Density-functional-theory (DFT) calculations (Gaussian program, B3LYP/6-31+G(d,p) level of theory) were performed for the dyes **1**-**4**. The energy-minimized structures of the dyes **2**-**4** show a nearly perpendicular positioning of the isoquinoline ring with respect to the aryl residue (tilt angles: 86.7º for **2**, 84.6º for **3**, and 86.5º for **4**). The calculated distance between the isoquinolinyl N and the boronic acid ester B atom is between 3.52 and 3.55 Å for these three dyes. This distance is slightly larger than the sum of the van-der-Waals radii of B (1.92 Å) and N (1.55 Å),[24] indicating the absence of interaction between the Lewis acid and base centers. In the case of dye **1** the optimized geometry shows a tilt angle of 59.0º and a lower distance between B and N (3.21 Å). This value is lower than the sum of the van-der-Waals radii of the atoms, supporting the notion of the formation of an intramolecular Lewis pair. These conclusions are corroborated by ^{11}B NMR spectroscopy (see Appendix C), showing the typical signals for tri-coordinated boron for the dyes **2**-**4** and a tetra-coordinated situation for dye **1**.

The contour plots of the frontier molecular orbitals (see Appendix C) illustrate that for the dyes **1**-**3** the HOMO (highest occupied molecular orbital) is located on the amino-substituted aryl electron-donor moiety. In contrast, the LUMO (lowest unoccupied molecular orbital) is located on the isoquinoline residue, which is thereby functioning as electron acceptor in the ICT process. For dye **4**, the HOMO is located on the piperazinyl-anthryl donor moiety and the LUMO on the borylated anthryl electron-acceptor residue. This hints on more localized transitions leading to the lowest energy excited state. This dye shows also a comparably reduced energy gap of *ca*. 3.2 eV, which is in accordance with the observation of the most red-shifted fluorescence emission in the investigated series.

5.5 Addition of Protons

The dyes are designed to allow a sequential protonation (see above). In the UV/vis absorption spectra corresponding to the titrations of the dyes with CF_3SO_3H clear isosbestic points for the orthogonal protonation steps are observed (see example of dye **1** in Figure 5.3). This hints on well-defined equilibria in the different phases of the titration. It is anticipated that the lateral aliphatic amino function is able to engage in electronic interactions with the excited ICT state of the dye, possibly via PET; see Scheme 5.2.

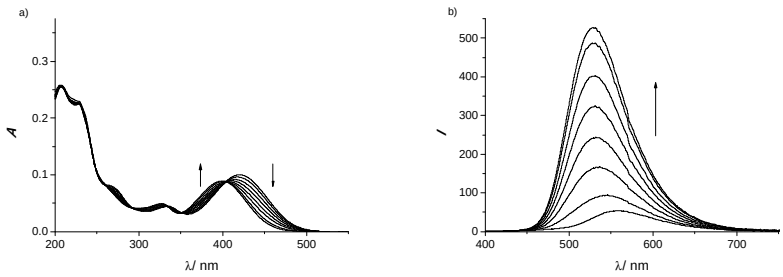

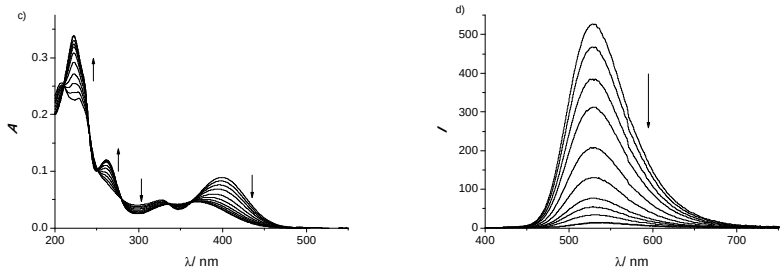

Figure 5.3. UV/vis absorption and fluorescence titration of dye **1** (8.2 µM) with CF_3SO_3H in acetonitrile; a) UV/vis spectra (0-1.0 equiv CF_3SO_3H), b) UV/vis spectra (1.0-2.1 equiv CF_3SO_3H), c) fluorescence spectra (0-1.0 equiv CF_3SO_3H); d) fluorescence spectra (1.0-2.1 CF_3SO_3H).

For dye **1**, the electron-donating methyl-substituted piperazinyl N atom is first protonated upon acid addition, which leads to the blocking of PET and consequently an increase of fluorescence is observed. In consequence, the fluorescence quantum yield increases (factor of *ca*. 6) and the lifetime shows the same trend. The fluorescence of the monoprotonated dye **1** is blue-shifted by *ca*. 30 nm due the sharing of the proton between the N atoms of piperazinyl and the consequent lowering of the electron donor strength of the aryl nitrogen.[19] A similar trend is observed for dye **2** and **4** (see Table 5.1). For the dyes **2** and **3** the protonation leads to an enhancement of fluorescence, but smaller than for the dye **1**. For dye **4** there is no alteration of the quantum yield. All fluorescence changes upon protonation are easily detected with the naked eye (Figure 5.4).

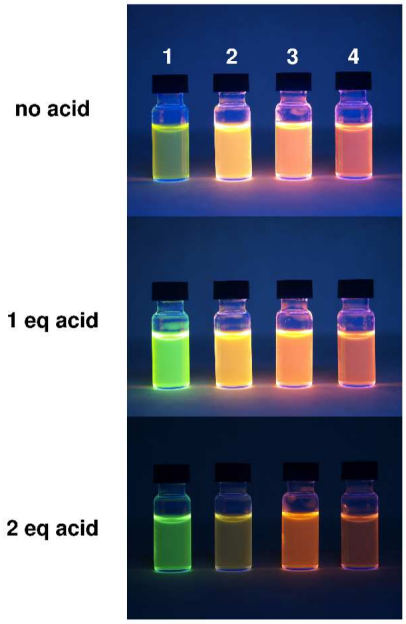

Figure 5.1. Color perception and brightness of the dyes **1**-**4** in the absence of acid and in the presence of one or two equivalents CF_3SO_3H in acetonitrile solutions.

The second acid equivalent protonates the isoquinolinyl moiety and results in practically quantitative quenching of the ICT fluorescence for all dyes. The quenching can be attributed to the increasing acceptor strength of the protonated isoquinoline that leads to a rather low-lying ICT state (see also discussion in Chapter 4).

For dye **3** a third protonation with an excess (20 equivalents) of acid was observed and the emission maximum of the new species was blue-shifted to 450 nm. This spectral displacement is indicative of an energetically destabilized ICT state due to the excessive weakening of the electron donor strength of the fully protonated aromatic N.

5.6 Multi-Level Logic Switches

The investigated dyes and their photophysical behavior are interesting for the implementation of multivalued logic. Usually logic switches distinguish between two states: *high* (binary 1) and *low* (binary 0). However, the dyes **1**-**4** are able to differentiate between more than two levels for the inputs and/or the output signals. In the case of ternary switching it is possible to obtain three signal levels, for example, *low* (0), *medium* (1), and *high* (2).

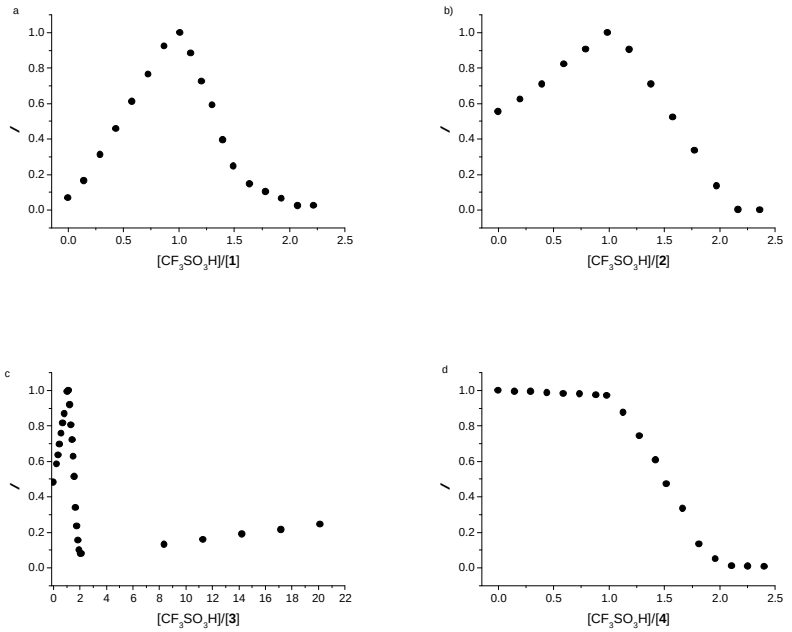

Figure 5.5. Fluorescence titration curves of dyes a) **1**, b) **2**, c) **3**, d) **4** upon addition of CF_3SO_3H.

The fluorescence behavior of the different dyes upon protonation is summarized in Figure 5.5 for the reading of the emission signal at a "strategic" wavelength. Dye **1** behaves as *off-on-off* fluorescence switch with three proton input levels (*low*, *medium*, and *high*); see Table 5.1 and 5.2. Alternatively, this dye can be discussed as XOR logic gate with

degenerate proton inputs.[26] For this logic gate the presence of either proton input results in a high fluorescence, while the absence or simultaneous presence of both inputs yields a low fluorescence signal.
Dye **2** shows a medium fluorescence level in the absence of protons. Upon protonation the fluorescence is further increased, but the second equivalent of acid quenches the fluorescence quantitatively. This integrates the behavior of a *medium-on-off* switch with three discrete emission output levels that can be assigned to 1, 2, and 0, respectively.

Table 5.2. Truth table for the multivalued switching of the dyes **1**-**4**.

H^+ *input* [a]	*Fluorescence Output*			
	Dye **1** (λ_{obs} = 530 nm) [b]	Dye **2** (λ_{obs} = 576 nm) [b]	Dye **3** (λ_{obs} = 526 nm) [c, d]	Dye **4** (λ_{obs} = 622 nm) [b, d]
0	0	1	2	1
1	1	2	3	1
2	0	0	0	0
3			1	
Output	**binary** *off-on-off*	**ternary** *medium-on-off*	**quaternary**	**binary** *on-off*

[a] The inputs levels 0, 1, and 2 correspond to the same number of CF_3SO_3H equivalents; level 3 (only applicable to dye **3**) corresponds to 20 equiv CF_3SO_3H. [b] Fluorescence maximum of the monoprotonated form of the dye. [c] Monitored at a wavelength where all forms (**3**, $\mathbf{3H^+}$, $\mathbf{3H_2^{2+}}$, and $\mathbf{3H_3^{3+}}$) emit. [d] Monitoring the fluorescence output for **3** at 600 nm ($\mathbf{3H^+}$) or for dye **4** at 580 nm (away from the maximum of any implied form) yields the reconfiguration of the switch toward a *medium-on-off* output signaling pattern.

Dye **3** is a special case due to the possibility of three protonation steps that are well differentiated by the emission quantum yields of the formed species and/or their different fluorescence maxima. At the wavelength of 526 nm, where all four forms have an emission signal, a four-level response (quaternary logic corresponding to 0, 1, 2, 3) can be observed: **3** (level 2), $\mathbf{3H^+}$ (level 3), $\mathbf{3H_2^{2+}}$ (level 0), and $\mathbf{3H_3^{3+}}$ (level 1) (Figure 5.5, Table 5.2). Such switching behavior integrating four output levels is

extremely rare and only one other example is known in the literature.[27] Alternatively, the switch can be interpreted as *on-off-on'* device, where the two *on* situations correspond to different emission wavelengths (e.g., 600 nm and 450 nm). The implementation of such behavior has been described recently as non-trivial.[28,29]

Finally, dye **4** is an example of a conventional *on-off* binary switch upon addition of two equivalents of protons for the observation wavelength of 622 nm (emission maximum of $\mathbf{4H^+}$). At other observation wavelengths (for example 580 nm) a *medium-on-off* signaling pattern according to a ternary output response is obtained (see Table 5.2).

5.7 Conclusion

In summary, a series of borylated arylisoquinoline dyes that feature aromatic amino substitution and lateral aliphatic amino groups as electron donors was photophysically characterized. These fluorophores are based on ICT processes and their emission and UV/vis absorption can be tuned by multiple and orthogonal protonation. This provides a convenient tool for achieving pH-induced fluorescence switching consisting in enhancement as well as quenching.

In general, the protonation of the lateral amino group leads to an increase of emission quantum yield and a somewhat blue-shifted emission. The second protonation at the isoquinoline moiety yields practically quantitative fluorescence quenching. However, for dye **3** even a third protonation was possible which was indicated by a strongly blue-shifted new emission band. The mechanistic explanation of the observed fluorescence modulation relies on the involvement of PET and the destabilization/stabilization of ICT states.

The fluorescence modulation upon addition of protons can be read as output signal and leads to the interpretation of multi-level logic switching including *off−on−off*, ternary, and quaternary responses.

5.8 References

[1] de Silva, A. P.; Gunaratne, H. Q. N.; Gunnlaugsson, T.; Huxley, A. J. M.; McCoy, C. P.; Rademacher, J. T.; Rice, T. E. *Chem. Rev.* **1997**, *97*, 1515.

[2] Martínez-Máñez, R.; Sancenón, F. *Chem. Rev.* **2003**, *103*, 4419.

[3] Anslyn, E. V. *J. Org. Chem.* **2007**, *72*, 687.

[4] de Silva, A. P.; Vance, T. P.; West, M. E. S.; Wright, G. D. *Org. Biomol. Chem.* **2008**, *6*, 2468.

[5] Guo, Z.; Shin, I.; Yoon, J. *Chem. Commun.* **2012**, *48*, 5956.

[6] de Silva, A. P.; Uchiyama, S. *Nat. Nanotechnol.* **2007**, *2*, 399.

[7] Pischel, U. *Angew. Chem. Int. Ed.* **2007**, *46*, 4026.

[8] Credi, A. *Angew. Chem. Int. Ed.* **2007**, *46*, 5472.

[9] Szaciłowski, K. *Chem. Rev.* **2008**, *108*, 3481.

[10] Tian, H. *Angew. Chem. Int. Ed.* **2010**, *49*, 4710.

[11] Andréasson, J.; Pischel, U. *Chem. Soc. Rev.* **2010**, *39*, 174.

[12] de Silva, A. P. *Molecular Logic-based Computation*; The Royal Society of Chemistry: Cambridge, **2013**.

[13] de Ruiter, G.; Motiei, L.; Choudhury, J.; Oded, N.; van der Boom, M. E. *Angew. Chem. Int. Ed.* **2010**, *49*, 4780.

[14] de Silva, A. P.; Gunaratne, H. Q. N.; McCoy, C. P. *Chem. Commun.* **1996**, 2399.

[15] de Silva, S. A.; Zavaleta, A.; Baron, D. E.; Allam, O.; Isidor, E. V.; Kashimura, N.; Percarpio, J. M. *Tetrahedron Lett.* **1997**, *38*, 2237.

[16] Albelda, M. T.; Bernardo, M. A.; García-España, E.; Godino-Salido, M. L.; Luis, S. V.; Melo, M. J.; Pina, F.; Soriano, C. *J. Chem. Soc., Perkin Trans. 2* **1999**, 2545.

[17] de Silva, S. A.; Amorelli, B.; Isidor, D. C.; Loo, K. C.; Crooker, K. E.; Pena, Y. E. *Chem. Commun.* **2002**, 1360.

[18] Callan, J. F.; de Silva, A. P.; Ferguson, J.; Huxley, A. J. M.; O'Brien, A. M. *Tetrahedron* **2004**, *60*, 11125.

[19] Pais, V. F.; Remón, P.; Collado, D.; Andréasson, J.; Pérez-Inestrosa, E.; Pischel, U. *Org. Lett.* **2011**, *13*, 5572.

[20] de Ruiter, G.; Motiei, L.; Choudhury, J.; Oded, N.; van der Boom, M. E. *Angew. Chem. Int. Ed.* **2010**, *49*, 4780.

[21] Khalili, F.; Henni, A.; East, A. L. L. *J. Chem. Eng. Data* **2009**, *54*, 2914.

[22] Zieliński, W.; Kudelko, A. *Arkivoc* **2005**, *(v)*, 66.

[23] Pais, V. F.; El-Sheshtawy, H. S.; Fernández, R.; Lassaletta, J. M.; Ros, A.; Pischel, U. *Chem. Eur. J.* **2013**, *19*, 6650.

[24] Mantina, M.; Chamberlin, A. C.; Valero, R.; Cramer, C. J.; Truhlar, D. G. *J. Phys. Chem. A* **2009**, *113*, 5806.

[25] Rehm, D.; Weller, A. *Ber. Bunsenges. Phys. Chem.* **1969**, *73*, 834.

[26] Credi, A.; Balzani, V.; Langford, S. J.; Stoddart, J. F. *J. Am. Chem. Soc.* **1997**, *119*, 2679.

[27] Di Pietro, C.; Guglielmo, G.; Campagna, S.; Diotti, M.; Manfredi, A.; Quici, S. *New J. Chem.* **1998**, *22*, 1037.

[28] Luxami, V.; Kumar, S. *Tetrahedron Lett.* **2007**, *48*, 3083.

[29] Amendola, V.; Bergamaschi, G.; Boiocchi, M.; Fabbrizzi, L.; Mosca, L. *J. Am. Chem. Soc.* **2013**, *135*, 6345.

Chapter 6

Summary and Outlook

6. Summary and Outlook

6.1 Summary

The work described in this thesis focuses on the development and design of fluorescent molecules for applications as sensors and logic switches.

Chapter 1 presents a concise review of molecular systems that mimic basic and advanced logic device functions by using chemical species or photonic signals as inputs and generating the corresponding optical outputs.

Chapter 2 outlines the objectives of this thesis.

Chapter 3 describes a new fluorescent triad with two receptors that can be addressed by degenerate proton inputs in an orthogonal manner. The designed 4-aminonaphthalimide derivative allows the proposal of the first example of a molecular device with T-latch characteristics. This simple molecule is a switch which upon single application of an input changes to the *on* state and that is set back to the *off* state by a second subsequent input of equal chemical nature. The two receptors, with different pK_a values, provide the possibility of a stepwise protonation. The first protonation leads to an increase of fluorescence by blocking of PET, and the second equivalent triggers emission quenching that is presumably caused by hydrogen-bonding interaction of quinolinium NH+ with the imide carbonyl C=O. The different protonation states can be easily reset to the unprotonated initial state by neutralization with a strong base.

Chapter 4 describes a new series of borylated arylisoquinolines featuring systematic variations of their structural and electronic properties. The fluorophores were tested for potential applications as molecular switches with protons and fluoride as chemical inputs. The compounds with weak electron-donating aryl residues show fluorescence emission in the blue-shifted spectral region. On other hand, strong electron-donating aryl

moieties lead to emission bands in the red spectral region. The observed fluorescence is based on internal charge transfer (ICT), involving the aryl residue as donor and the isoquinoline part of the molecule as acceptor. The protonation causes an enhancement of fluorescent in compounds with low ICT character, and a quenching for compounds with pronounced ICT character. On other hand, the formation of a fluoroboronate adduct with fluoride ions leads to strong fluorescence quenching for all compounds.

For the non-borylated model compounds the emission wavelength is blue-shifted and the emission quantum yield is reduced. By observation of the different photophysical properties of the models and the borylated compounds it is possible to conclude that the boron substituent plays an important role in establishment of the emissive properties.

Chapter 5 presents the photophysical characterization of pH-switchable fluorescent borylated arylisoquinolines which are based on ICT and PET processes. The borylated compounds feature an aromatic amino substitutent and a lateral aliphatic amino group as electron donors. All dyes present high fluorescent quantum yields and cover a broad emission range. Emission and absorption depend on the amino substitution, the degree of π-conjugation of the aryl residue, and the presence of the boron substituent. The presence of the different electron-donating basic groups enables multiple and orthogonal protonation of the compounds. When the lateral amino is protonated then the quantum yield increases in most cases. This is contrasted by a strong fluorescence quenching upon the second protonation at the isoquinoline. For one compound a third protonation step was observed. Reading fluorescence responses as outputs and addition of protons as input signals, the molecules behave as *off-on-off* and *on-off-on'* switches and as well as ternary and quaternary switches. The investigated series provides an interesting toolbox for the realization of these non-trivial logic operations.

6.2 Outlook

Among other results in this thesis a new class of fluorophores was discovered and progress was made in the understanding of the photophysical behavior of these borylated arylisoquinolines. The structural motif is extremely versatile so that many more applications beside the herein discussed uses as sensors and molecular logic devices can be imagined. These include the exploitation of these heterobiaryls as molecular thermometers, for which first promising experiments have been performed recently. Furthermore, the exploitation of the boronic acid motif as handle for bioconjugation to carbohydrate structures could be explored. The high fluorescence quantum yields and spectrally differentiated fluorescence emission of some members of this family may open perspectives for their use in fluorescence microscopy. The push-pull character of the chromophores is likely to result in high two-photon-absorption cross sections, which is a pre-condition for their use in two-photon-excitation confocal microscopy. Finally, the boronic acid motif could be employed for the supramolecular assembly of these chromophores and the creation of new functional structures.

6.3 Conclusiones

El trabajo descrito en esta tesis se centra en el diseño y desarrollo de moléculas fluorescentes para aplicaciones como sensores e interruptores lógicos.

El capítulo 1 presenta una revisión concisa de los sistemas moleculares que imitan las funciones básicas y avanzadas de dispositivos lógicos utilizando especies químicas o señales fotónicas como *inputs* y generando los *inputs* ópticos correspondientes.

El capítulo 2 resume los objetivos de la tesis.

El capítulo 3 describe una nueva tríada fluorescente con dos grupos diferentes que funcionan como receptores de protones. El derivado de 4-

aminonaftamilida, hizo posible que se llevara a cabo el primer ejemplo de un dispositivo molecular con las características de un T-latch. La intensidad de la fluorescencia de la molécula funciona como un interruptor en el que se consigue el estado de encendido después de la primera aplicación de un compuesto y vuelve al estado apagado con una segunda adición del mismo compuesto u otro con la misma naturaleza. Al tener dos receptores con diferentes valores de pK_a se proporciona la posibilidad de una protonación paso a paso. De esta manera, la primera protonación condujo a un aumento de la fluorescencia mediante el bloqueo de la transferencia electrónica fotoinducida, y la adición del segundo equivalente llevó a una bajada de emisión que fue presumiblemente causada por la interacción del enlace de hidrógeno del quinolinium NH^+ con el carbonilo C=O de la imida. Estos estados de protonación se pueden restablecer fácilmente utilizando una base fuerte.

El capítulo 3 describe una nueva serie de arilisoquinolinas boriladas con variaciones sistemáticas de sus propiedades estructurales y electrónicas. Los fluoróforos se ensayaron para potenciales aplicaciones como interruptores moleculares con protones y fluoruro como insumos químicos.

Los compuestos con débiles restos arilo donadores de electrones mostraron emisión de fluorescencia en la región azul. Por otra parte, fuertes restos arilo donadores de electrones llevaron a bandas de emisión en la región espectral roja. La fluorescencia observada se basa en la transferencia interna de carga (TIC), que implica al residuo arilo como donante a la isoquinolina, parte aceptora de la molécula. La protonación provocó un aumento de la fluorescencia en compuestos con bajo carácter TIC, y una bajada de fluorescencia de los compuestos con carácter TIC pronunciado. Por otra parte, la formación de un aducto de Lewis con aniones fluoruro condujo a una fuerte inhibición de la fluorescencia para todos los compuestos.

Para los compuestos modelo, la longitud de onda de emisión se movió para el azul y el rendimiento cuántico de emisión se redujo. Observando las diferencias entre las propiedades fotofísicas de los modelos y de los

compuestos borilados fue posible concluir que el sustituyente boro tenía un papel importante en el establecimiento de las propiedades emisivas.

El capítulo 4 presenta la caracterización fotofísica de arilisoquinolinas boriladas fluorescentes de pH dependientes que se basan en procesos TIC. Los compuestos borilados tenían una sustitución amino aromático y un grupo amino alifático lateral como donadores de electrones. Todos los colorantes presentan altos rendimientos cuánticos de fluorescencia y cubren un amplio rango de emisión. La emisión y la absorción dependen de la sustitución del grupo amino, del grado de la conjugación π del residuo arilo y de la presencia del sustituyente de boro. La presencia de los diferentes grupos básicos donadores de electrones permite la protonación múltiple y ortogonal. Cuando el amino lateral fue protonado el rendimiento cuántico se incrementó en la mayoría de los casos, pero la segunda protonación de la isoquinolina condujo a una fuerte atenuación de la fluorescencia. Para uno de los compuesto se observó un tercer paso de protonación. Si se leen las respuestas de fluorescencia como *outputs* y la adición de protones como *inputs*, la molécula se comporta como un interruptor *off-on-off* y on-*off-on,* así como ternario y cuaternario. La serie investigada proporciona una caja de herramientas interesante para la realización de estas operaciones lógicas no triviales.

Appendices

Appendices

Los artículos publicados en revistas científicas han sido retirados de este apartado de la tesis debido a las restricciones relativas a los derechos de autor. Dichos artículos han sido sustituidos por las referencias bibliográficas de más abajo, además si la UHU tiene suscripción a la versión electrónica de las revistas se añade un enlace que será de acceso restringido a miembros de la UHU.

Referencias bibliográficas:

- ***Off-On-Off Fluorescence Switch with T-Latch Function***

Pais, V. F.; Remón, P.; Collado, D.; Andréasson, J.; Pérez-Inestrosa, E.; Pischel, U. *Org. Lett.* **2011**, *13*, 5572-5575.

Enlace al texto complete del artículo (solo para miembros de la UHU):

http://pubs.acs.org/doi/ipdf/10.1021/ol202312n

- ***Borylated Arylisoquinolines: Photophysical Properties and Switching Behavior of Promising Tunable Fluorophores***

Pais, V. F.; El-Sheshtawy, H. S.; Fernández, R.; Lassaletta, J. M.; Ros, A.; Pischel, U. *Chem. Eur. J.* **2013**, *19*, 6650-6661.

Enlace al texto completo del artículo (solo para miembros de la UHU):

http://onlinelibrary.wiley.com/doi/10.1002/chem.201203887/pdf

- ***Preparation and pH-Switching of Fluorescent Borylated Arylisoquinolines for Multilevel Molecular Logic***

Pais, V. F.; Lineros, M.; López-Rodríguez, R.; El-Sheshtawy, H. S.; Fernández, R.; Lassaletta, J. M.; Ros, A.; Pischel, U. *J. Org. Chem.* **2013**, *78*, 7949-7961.

Enlace al texto completo del artículo (solo para miembros de la UHU):

http://pubs.acs.org/doi/ipdf/10.1021/jo401147t

Appendix D: *Curriculum Vitae*

CURRICULUM VITAE

BIOGRAPHICAL DATA

Name: **VÂNIA CRISTINA FERNANDES PAIS**
Birthday: 02.09.1984
Birthplace: Juromenha (Nossa Senhora do Loreto), Portugal
Marital Status: Single
Contact (Work): Department of Chemical Engineering, Physical Chemistry, and Organic Chemistry, University of Huelva, Campus de El Carmen s/n, E-21071 Huelva (Spain). E-mail: vaniacristina.fernandes@diq.uhu.es; Tel: +34 959 21 99 86/87

UNIVERSITY EDUCATION

2002 – 2007	Studies of Chemistry at the University of Évora, Portugal
19/12/2007	Diploma Degree in Chemistry; Thesis: "Synthesis of new organic ligands for *nonlinear optical complexes*", at the University of Évora, Portugal
14/08/2008	Master Degree in Applied Chemistry, at the University of Évora, Portugal
2009 – 2013	PhD studies at the University of Huelva, Spain

FELLOWSHIPS

2008 – 2009 Research Fellowship, CESAM at the University of Aveiro

2009 – 2013 PhD Fellowship of the *Junta de Andalucía*

PUBLICATIONS

Off-On-Off Fluorescence Switch with T-Latch Function

Pais, V. F.; Remón, P.; Collado, D.; Andréasson, J.; Pérez-Inestrosa, E.; Pischel, U. *Org. Lett.* **2011**, *13*, 5572-5575.

An Electronic Nose Based on Coated Piezoelectric Quartz Crystals to Certify Ewes' Cheese and to Discriminate Between Cheese Varieties

Pais, V. F.; Oliveira, J. A. B. P., Gomes, M. T. S. R. Sensors (Basel) 2012, 12, 1422-1436.

Information Processing with Molecules—Quo Vadis?

Pischel, U.; Andréasson, J.; Gust, D.; Pais, V. F. *ChemPhysChem* **2012**, *14*, 28-46.

Borylated Arylisoquinolines: Photophysical Properties and Switching Behavior of Promising Tunable Fluorophores

Pais, V. F.; El-Sheshtawy, H. S.; Fernández, R.; Lassaletta, J. M.; Ros, A.; Pischel, U. *Chem. Eur. J.* **2013**, *19*, 6650-6661.

Unconventional Fluorescence Quenching in Naphthalimide-Capped CdSe/ZnS Nanoparticles

Aguilera-Sigalat, J.; Pais, V. F.; Doménech-Carbó, A.; Pischel, U.; Galian, R. E.; Pérez-Prieto, J. *J. Phys. Chem. C* **2013**, *117*, 7365-7375.

Preparation and pH-Switching of Fluorescent Borylated Arylisoquinolines for Multilevel Molecular Logic

Pais, V. F.; Lineros, M.; López-Rodríguez, R.; El-Sheshtawy, H. S.; Fernández, R.; Lassaletta, J. M.; Ros, A.; Pischel, U. *J. Org. Chem.* **2013**, *78*, 7949-7961.

Highly Sensitive Organic Molecular Fluorescent Thermometers Based on Borylated Arylisoquinolines

Pais, V. F.; Lassaletta, J. M.; Fernández, R.; El-Sheshtawy, H. S.; Ros, A.; Pischel, U. *to be submitted*.

CONFERENCES CONTRIBUTIONS

New Organic Ligands for Nonlinear Optical Complexes

Pais, V. F.; Teixeira, A. P. S.; Robalo, M. P.; Garcia, M. H.; Piedade, M. F. M.; Duarte, M. T.; Dias, A. R., Book of Abstracts *7th Portuguese National Meeting of Organic Chemistry, 1st Luso-French Symposium*, July 16-18, **2007**, Lisbon, Portugal. (Poster)

Synthesis and Characterization of Novel Octahedral $[FeH(DPPE)_2(NCR)][PF_6]$ Compounds

Teixeira, A. P. S.; Falcão, A.; Pais, V. F.; Robalo, M. P.; Garcia, M. H., Book of Abstracts *XXI National Meeting of SPQ*, June 11-13, **2008**, Oporto, Portugal. (Poster)

Synthesis and Characterization of Nitrile Ligands Towards Molecular Wires

Pais, V. F.; Robalo, M. P.; Garcia, M. H.; Piedade, M. F. M.; Duarte, M. T.; Teixeira, A. P. S.; Book of Abstracts 9th *International Conference on*

Heteroatom Chemistry, June 30th to July 4th, **2009**, Oviedo, Spain. (Poster)

Following Milk Coagulation with Animal and Vegetal Rennet using an Acoustic Wave Sensor

Pais, V. F; Oliveira, J. A. B. P.; Gomes, M. T. S. R., Book of Abstracts *European Conference on Analytical Chemistry 2009 (EUROANALYSIS)*, September 6-10, **2009**, Innsbruck, Austria. (Poster)

Development of an Electronic Nose to Discriminate Cheese Variety

Pais, V. F; Oliveira, J. A. B. P.; Gomes, M. T. S. R., Book of Abstracts *4th International Symposium on Recent advances in food analysis (RAFA)*, November 4- 6, **2009**, Prague, Czech Republic. (Poster)

Photophysical Studies of the Interaction of Nitroaniline Ligands with Quantum Dots

Pais, V. F.; Pischel, U., Book of Abstracts *10th National Meeting of Photochemistry (10ENF)*, *Sociedade Portuguesa de Químic*a, December 9-10, **2010**, Porto, Portugal. (Poster)

A Molecular Logic Memory Device

Pais, V. F.; Remón, P.; Collado, D.; Andréasson, J.; Pérez-Inestrosa, E.; Pischel, U., Book of Abstracts *III Jornadas Ibéricas de Fotoquímica and X Congreso de Fotoquímica*, September 4-7, **2011**, Granada, Spain. (Poster)

Pyridinium Porphyrins and Their Host-Guest Interactions with Cucurbituril Macrocycles

Costa, D. C. S.; Pais, V. F.; Silva, A. M. S.; Cavaleiro, J. A. S.; Pischel, U.; Tomé, J. P. C., Book of Abstracts *3rd Portuguese Young Chemists Meeting (PYCHEM 2012)*, **2012**, May 9-11, Oporto, Portugal. (Poster)

OFF-ON-OFF Fluorescence Switch with T-Latch Function

Pais, V. F.; Remón, P.; Collado, D.; Andréasson, J.; Pérez-Inestrosa, E.; Pischel, U., Book of Abstracts *XXIV IUPAC Symposium on Photochemistry*, July 15-20, **2012**, Coimbra, Portugal. (Poster)

Evaluation of Photoelectron Transfer in OFF-ON-OFF Fluorescence Switch

Collado, D.; Najera, F.; Pérez-Inestrosa, E.; Pischel, U.; Pais, V. F.; Remón, P., Book of Abstracts *XXIV IUPAC Symposium on Photochemistry*, July 15-20, **2012**, Coimbra, Portugal. (Oral Communication)

Amine-Induced Changes in the Optical Features of Naphthalimide Coated CdSe/ZnS Nanohybrids

Aguilera-Sigalat, J.; Domenech, A.; Pais, V. F.; Pischel, U.; Galian, R. E.; Pérez-Prieto, J., Book of Abstracts *XXIV IUPAC Symposium on Photochemistry*, July 15-20, **2012**, Coimbra, Portugal. (Poster)

Pyridinone Phthalocyanines and Their Host-Guest Complexes with Cucurbit-7-uril

Lourenço, L. M. O.; Pais, V. F.; Neves, M. G. P. M. S.; Cavaleiro, J. A. S.; Pischel, U.; Tomé, J. P. C., Book of Abstracts *XXIII Encontro Nacional da SPQ*, June 12-14, **2013**, Aveiro, Portugal. (Poster)

Bor-ON or OFF: An Unexpected Discovery of a Versatile Class of Fluorescent Organoboron Switches and Their Applications

Pischel, U.; Pais, V. F.; Ros, A.; Fernández, R.; Lassaletta, J. M.; El-Sheshtawy, H. S., Book of Abstracts *XXXIV Reunión Bienal de la Real Sociedad Española de Química*, September 15-18, **2013**, Santander, Spain. (Oral Communication)

PROFESSIONAL MEMBERSHIPS

Portuguese Society of Chemistry (SPQ) – since 2006